CALIFORNIA ENERGY COMMISSION

CALIFORNIA NATURAL RESOURCES AGENCY

ENERGY RESEARCH AND DEVELOPMENT DIVISION

FINAL PROJECT REPORT

Pilot Testing of Isothermal Compression

June 2024 | CEC-500-2024-071

PREPARED BY:

Luke Bingham, Engineer
Rob Kamisky, R&D Manager
Carlos Ortiz, Engineer
Jason Stair, Senior Engineer
Gas Technology Institute

Todd Thompson, CEO
Chris Finley, VP Engineering
Hans Shillinger, COO
Christophe Duchateau, Principal Engineering Scientist
Carnot Compression, Inc.
Primary Authors

Anish Gautam, P.E.
Project Manager
California Energy Commission

Agreement Number: EPC-16-046

PREFACE

The California Energy Commission's (CEC) Energy Research and Development Division supports energy research and development programs to spur innovation in energy efficiency, renewable energy and advanced clean generation, energy-related environmental protection, energy transmission, and distribution and transportation.

In 2012, the Electric Program Investment Charge (EPIC) was established by the California Public Utilities Commission to fund public investments in research to create and advance new energy solutions, foster regional innovation, and bring ideas from the lab to the marketplace. The EPIC Program is funded by California utility customers under the auspices of the California Public Utilities Commission. The CEC and the state's three largest investor-owned utilities—Pacific Gas and Electric Company, San Diego Gas and Electric Company, and Southern California Edison Company—were selected to administer the EPIC funds and advance novel technologies, tools, and strategies that provide benefits to their electric ratepayers.

The CEC is committed to ensuring public participation in its research and development programs that promote greater reliability, lower costs, and increase safety for the California electric ratepayer and include:

- Providing societal benefits.
- Reducing greenhouse gas emission in the electricity sector at the lowest possible cost.
- Supporting California's loading order to meet energy needs first with energy efficiency and demand response, next with renewable energy (distributed generation and utility scale), and finally with clean, conventional electricity supply.
- Supporting low-emission vehicles and transportation.
- Providing economic development.
- Using ratepayer funds efficiently.

For more information about the Energy Research and Development Division, please visit the CEC's research website (www.energy.ca.gov/research/) or contact the Energy Research and Development Division at ERDD@energy.ca.gov.

ABSTRACT

Industrial air compressors are estimated to consume more than 12 percent of California's manufacturing electricity consumption annually yet estimates show that only 10 to 15 percent of the energy used to compress air translates to useful output. Carnot Compression Inc. (Carnot) developed, tested, and demonstrated an isothermal compression technology intended to improve the energy efficiency of compressed air systems. Increasing the percentage of useful work output of compressed air systems by managing these inefficiencies can decrease demand for electricity in California's industrial sector as well as in the agricultural, water, and commercial business sectors, thereby supporting state mandates to reduce planet-warming emissions 40 percent below 1990 levels by 2030 and achieve carbon neutrality by 2045.

A detailed engineering design process informed fabrication of Carnot's first fully integrated prototype, which was tested in a laboratory setting and subsequently installed and monitored at a field test location.

Flow rates during lab testing were below the targeted capacity and consequently below the monitoring system's flow cutoff, prompting a change in the measurement approach for field testing.

More than 115.5 and 155.6 hours of compressor run-time in the lab and the field, respectively, produced a significant volume of data, from which 571 compression events were selected, with flow rates of 0.63 actual cubic feet per minute at inlet conditions. Specific power was measured to be 3,091 kilowatts per 100 actual cubic feet per minute at inlet conditions, and isentropic efficiency was measured to be approximately 0.31 percent.

Although the alpha version compressor did not meet the efficiency levels of currently available commercial products, opportunities for improving system performance were identified and are being incorporated into the beta version compressor. Performance results of the prototype, environmental data for wastewater composition, sound levels, and vibration are also provided to inform future design considerations for commercialization.

Keywords: isothermal, compressor, isentropic efficiency, heat of compression, industrial compressor, compressed air, polytropic index

Please use the following citation for this report:

Bingham, Luke, Carlos Ortiz, Rob Kamisky, Hans Shillinger, Christophe Duchateau. 2022. *Pilot Testing of Isothermal Compression*. California Energy Commission. Publication Number: CEC-500-2024-071.

TABLE OF CONTENTS

LIST OF FIGURES

LIST OF TABLES

Executive Summary

Problem Statement/Background

Gas compression in industry standard compressors typically occurs as an adiabatic process, meaning that heat resulting from the compression of gases (e.g., heat of compression) is not transferred to the environment during compression. The heat of compression increases the work needed to compress gases to higher pressures and contributes to the friction of moving parts. Without accounting for line losses or poorly designed systems, estimates show that only 10 to 15 percent of the mechanical work used for compressing air translates to useful work output for compressed air systems (Compressed Air & Gas Institute, 2021). In 2006, industrial compressor motors were estimated to account for 1,122 terawatt-hours of electricity consumed globally — which amounted to between 15.6 and 16.3 percent of all motor-driven electricity consumption worldwide (Waide and Brunner, 2011). In California, industrial air compressors are estimated to consume more than 12 percent (approximately 5,400 gigawatt-hours) of annual manufacturing electricity consumption. Increasing the percentage of useful work output of compressed air systems by managing inefficiencies such as those caused by the heat of compression can have a far-reaching impact in reducing the demand for electricity, not only in California but across the globe, thereby supporting state mandates to reduce planet-warming emissions 40 percent below 1990 levels by 2030 and achieve carbon neutrality by 2045.

In addition, because these energy costs are estimated to account for approximately 75 percent of the lifetime cost of industrial air compressor ownership, improving the efficiency of compressed air systems would lower the cost for system owners.

Project Purpose

The purpose of this research was to fund the development, lab testing, and field demonstration of an isothermal compression technology that improves the energy efficiency of compressed air systems, enabling reduced energy consumption primarily across the industrial sector, but also within the agricultural, water, and commercial business sectors.

Project Approach

A possible solution for addressing the heat of compression would be to compress the air via an isothermal process, in which the heat of compression is removed from the air/gas as it is compressed to maintain a steady temperature. Many existing technologies attempt to manage the heat of compression, typically by incorporating cooling systems using water, air, or oil.

Carnot Compression Inc. (Carnot) has designed and developed a near-isothermal compression system that uses water as a working fluid. Carnot's design leverages the specific heat capacity of water and the large surface area-to-volume ratios of entrained air volumes to approach isothermal compression, allowing heat transfer to occur nearly instantaneously as the air is compressed, thereby diminishing the increase in temperature of the compressed air.

Major Objectives

This project supported extensive engineering design to produce a working, field-deployable isothermal air compressor alpha prototype. The major goals for this research were to:

- Develop an advanced isothermal air compressor capable of efficiently compressing air in an industrial setting.
- Fabricate and test the prototype air compressor in a controlled laboratory setting and measure the performance to verify that the compressor reduces energy consumption compared to existing compressors.
- Install and test the prototype air compressor at a field site to demonstrate performance of the compressor under real-world conditions.
- Create a pathway to transfer technology to a commercially available product.

Installation and Testing Barriers

Commissioning the prototype at both the lab and the field sites yielded information on some minor installation barriers, which were easily addressed.

Testing barriers were more problematic, principally due to the flow metering. A large portion of the laboratory testing was spent troubleshooting the selected coriolis mass flow meter and the potential replacement thermal dispersion mass flow meter. Aside from the actual flow rate being near the cutoff value for the specified meter, additional issues related to in-line condensation caused false readings during testing. After troubleshooting the meter and verifying the issues with the project team and the manufacturer, a refrigerated dryer was added to the monitoring line and an indirect approach to approximate the mass flow rate was selected for processing data collected from the field site. Ultimately, the method was crosschecked against the replacement laminar flow element mass flow meter to confirm the validity of the approach.

Project Results

More than 115.5 and 155.6 hours of compressor run-time were obtained in the lab and the field, respectively. From the resulting field data, 571 compression events were selected that showed flow rates to be 0.63 actual cubic feet per minute at inlet conditions, delivered at 112.8 pounds per square gauge. Using this same data, specific power was measured to be 3091 kilowatts per 100 actual cubic feet per minute at inlet conditions in Grass Valley, California, and isentropic efficiency was measured to be approximately 0.31 percent.

While the compressor was shown to have an efficiency and capacity below the expected targets, the project was able to demonstrate that the prototype was able to reliably produce compressed air at commercially useful pressures in an isothermal manner for long durations. Lab and field testing produced data that was useful not only for the purposes of demonstrating the prototype's performance under both laboratory and real-world environments, but also for providing additional engineering design and commercialization considerations.

Advancing the Research to Market

The project supported the development of a production readiness plan and technology transfer via webinars, media publications, website creation, marketing videos, and conference events. Carnot also consulted with various industry contacts and initiated discussions with potential manufacturing partners.

Benefits to California

By removing the heat throughout the compression step, the energy required to compress air from near atmospheric pressure to approximately 100–150 pounds per square gauge can be reduced by 20 percent or more compared to commercial air compressors such as piston, screw, or scroll designs. These energy savings are expected to significantly improve the efficiency of industrial air compression. Carnot also believes that the technology can be applied to other compressor applications in the future, such as compression of natural gas in transmission and distribution systems, leading to additional energy savings across many industrial gas applications.

CHAPTER 1: Introduction

In California, industrial air compressors are estimated to consume more than 12 percent (approximately 5,400 gigawatt-hours) of annual manufacturing electricity consumption. Gas compression in industry standard compressors typically occurs as an adiabatic process, meaning that heat resulting from the compression of gases (e.g., heat of compression) is not transferred to the environment during compression. The heat of compression increases the work needed to compress gases to higher pressures and contributes to the friction of moving parts. Without accounting for line losses or poorly designed systems, estimates show that only 10 to 15 percent of the mechanical work used for compressing air translates to useful work output for compressed air systems (Compressed Air & Gas Institute, 2021). Increasing the percentage of useful work output of compressed air systems by managing inefficiencies such as those caused by the heat of compression can have a far-reaching impact in reducing the demand for electricity in California's industrial sector as well as the agricultural, water, and commercial sectors, thereby supporting state mandates to reduce planet-warming emissions 40 percent below 1990 levels by 2030 and achieve carbon neutrality by 2045.

The purpose of this research was to fund the development, lab testing, and field demonstration of an isothermal compression technology that improves the energy efficiency of compressed air systems, enabling reduced energy consumption primarily across the industrial sector, but also within the agricultural, water, and commercial business sectors.

The Gas Technology Institute (GTI) and Carnot Compression Inc. (Carnot) partnered to develop and test a novel, near-isothermal air compressor, enabling improved efficiency, maintenance, and reliability of air compression. This near-isothermal compressor, or Carnot Compressor, addresses the heat of compression problem by using a working liquid to compress a gas while actively removing the heat of compression throughout the compression process. By removing the heat throughout the compression step, the energy required to compress air from near atmospheric pressure to approximately 100–150 pounds per square gauge (psig) can be reduced by 20 percent or more compared to commercial air compressors such as piston, screw, or scroll designs. These energy savings are expected to significantly improve the efficiency of industrial air compression. Carnot also believes that the technology can be applied to other compressor applications in the future, such as compression of natural gas in transmission and distribution systems, leading to additional energy savings across many industrial gas applications.

Carnot overcame installation and testing barriers to obtain data from more than 115.5 and 155.6 hours of compressor run-time during the lab and the field, respectively. Although the compressor demonstrated an efficiency and capacity below the expected targets, the project demonstrated that the prototype could reliably produce compressed air at commercially useful pressures in an isothermal manner for long durations in both laboratory and real-world environments. The data is also useful for providing additional engineering design and commercialization considerations.

CHAPTER 2: Project Approach

Technology Overview

The Carnot compressor consists of one rotating component, the compressor drum, and one static component, the static vane return (SVR). The compressor drum houses the main components of the compressor, which include the compression channels, pressure plate, water balance chamber, and air harvest plate. The SVR is also housed within the compressor drum but is held static by an independent mount.

It should be noted that, in some iterations during this project, the role of the SVR was held by a turbine rotating more slowly than the compressor drum. This recirculation and energy recovery turbine required a transmission system to redirect its recovered power into the main compressor shaft, adding complexity to the system, which is the reason why it was abandoned in favor of the SVR.

Figure 1 shows a process diagram of the Carnot compressor and includes the flow path for both the water and the air within the system. The design of this compressor uses an internally recirculating water system (closed loop), while drawing in and compressing air through the air intake and harvesting it through the compressor shaft (open loop). The flow of water and air can be described by this sequence:

1. Water at ambient pressure enters the inner diameter of the compression cassette.
2. Centrifugal force causes the water to enter the inlet of the compression channels, where a certain amount of air is entrained.
3. The water and air emulsion flows through the compression channels toward the outer diameter of the compression cassette, where it exits the compression channels at the compressor's maximum operating pressure.
4. The air then separates from the emulsion, moves towards the center of the drum due to the higher density of the water, and is captured into separation chambers.
5. The pressurized air is harvested through the air harvest plate, into the hollowed compressor drive shaft, and finally to a storage tank.
6. With the SVR held static, water enters the SVR and is brought back to the center of the compressor drum at ambient pressure and high momentum, thus reducing the power required to spin the drum.
7. A small fraction of the water flow is diverted to an external water management loop for cooling and filtration and to adjust the amount of water in the drum.
8. The process then repeats.

Figure 1: Carnot Compressor Process Diagram (Simplified)

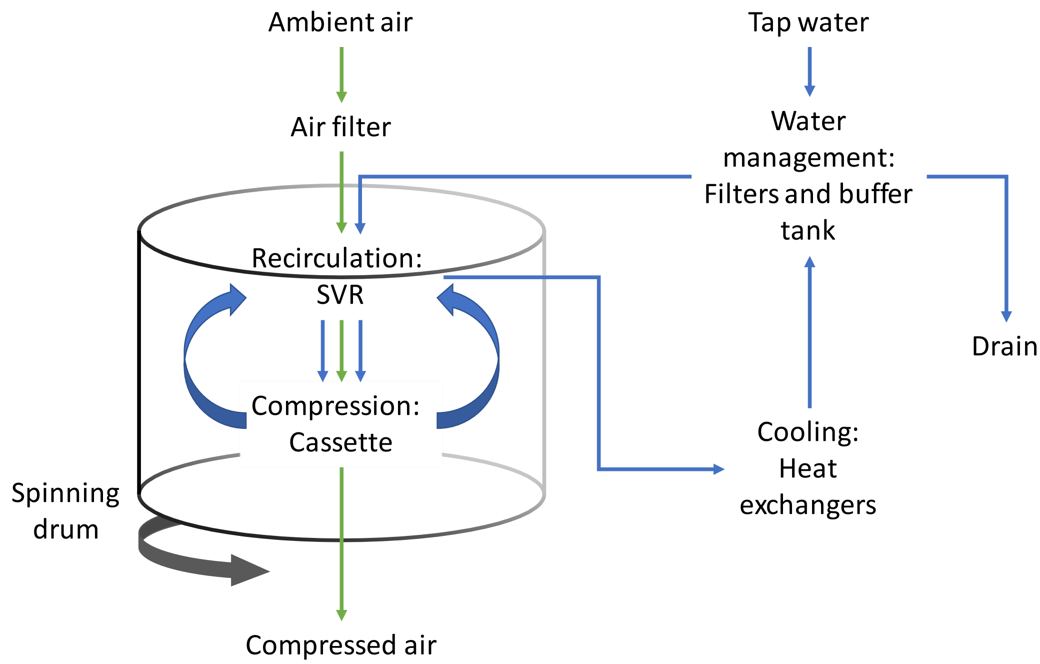

Simplified schematic of the Carnot Compressor process, from intake air and water to final compressed air product

Source: Carnot Compressor Inc.

Engineering Design

The prototype engineering and design process relied on a multiprong approach based on prototyping/testing, test data analysis, and models/simulations. The preliminary design consisted of prototyping using a test bed device named "FD2," which allowed the project team to develop the design targets for the field-deployable iteration of the Carnot isothermal compressor "FD3."

Much more detailed descriptions of the engineering and design process, along with the issues and corrections that occurred during the shake-down phase, can be found in the Preliminary Design Report and the Final Design Report documents submitted to the California Energy Commission as part of this project. The following sections provide a brief but detailed review of this engineering design process, and the following list summarizes the design objectives for the FD3 based upon the preliminary design work performed with the FD2 test bed.

FD3 Design Objectives

- Fully functional commercial-grade air compressor
- Automated operation and good reliability
- Air production: 25–30 actual cubic feet per minute at 100–125 psig
- Maximum footprint: 6′ x 6′ x 6′
- Motor sizing: three-phase 208–240/480 V (volt), 15 HP (horsepower)

Preliminary Design – FD2 Test Bed and Six-tube Device

The FD2 test bed allowed Carnot to test different designs for the entire system at full scale for various configurations and operational conditions. Additionally, a more focused test skid referred to as the "six-tube" device was also used at the beginning of the project, specifically for compression tube testing, as shown in Figure 2.

Figure 2: FD2 Test Bed and Six-tube Device

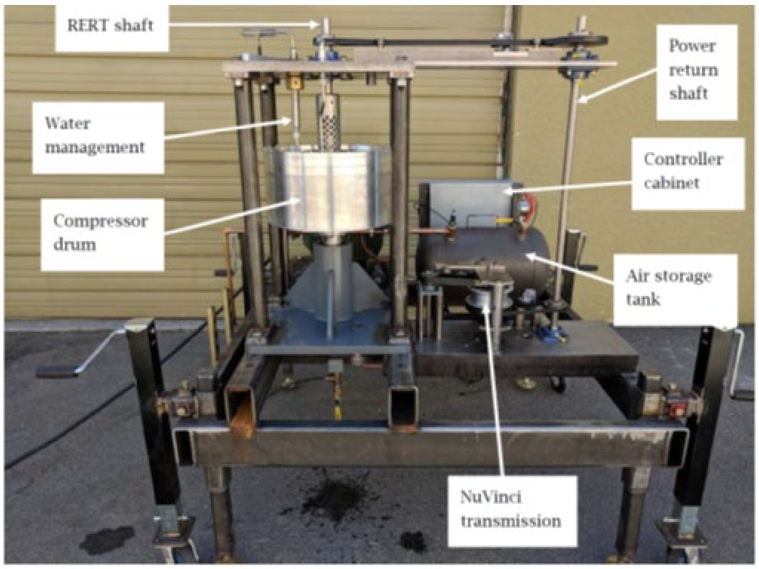

Carnot prototypes: FD2 test bed (left) and six-tube device (right)

Source: Carnot Compressor Inc.

The test data collected from the FD2 test bed was analyzed in an iterative manner to determine if a configuration, design, or operational change was beneficial to the overall efficiency of the system, as well as to help pinpoint areas of the system presenting the most potential for improvement. Along with traditional engineering analysis, the preliminary design effort also employed the use of computational fluid dynamics (CFD) simulations. This allowed for comparison of the predictive models against real-world test results, providing further insights into how to improve the compressor.

The preliminary design with the FD2 test bed and the six-tube skid specifically involved examining the following to aid in establishing design targets: emulsifier type, compression tube design, recirculation and energy recovery turbine design, heat management, water management, and overall system efficiency.

Compression Tube Design

Perhaps the most important part of the preliminary design was the study of the compression tubes themselves and the emulsifier design, as the gas/liquid ratio was shown to be one of the most impactful parameters in terms of efficiency and capacity. The team investigated using siphons, ejectors, and open/castellated tubes as options. The six-tube device was used to test 11 different tube geometries and configurations to examine the impact of the tube diameters and inlet design on the gas/liquid volume ratio.

During testing, it was determined that both the siphons and the ejectors were difficult to scale to the required dimensions and that the open/castellated tubes offered sufficiently high gas/liquid ratios with a lower head for the entering water. The tapered castellations (see Figure 3) offered some advantage to creating turbulence for smaller diameter tubes but ultimately the project team moved to simpler tubes of a larger diameter that produced less friction, with an angled tube entry providing the necessary turbulence (see Figure 4).

Figure 3: Tapered Castellated Tube Design

Design of the tapered castellated tube

Source: Carnot Compression Inc.

Figure 4: Computational Fluid Dynamic Modelling of Tube Design

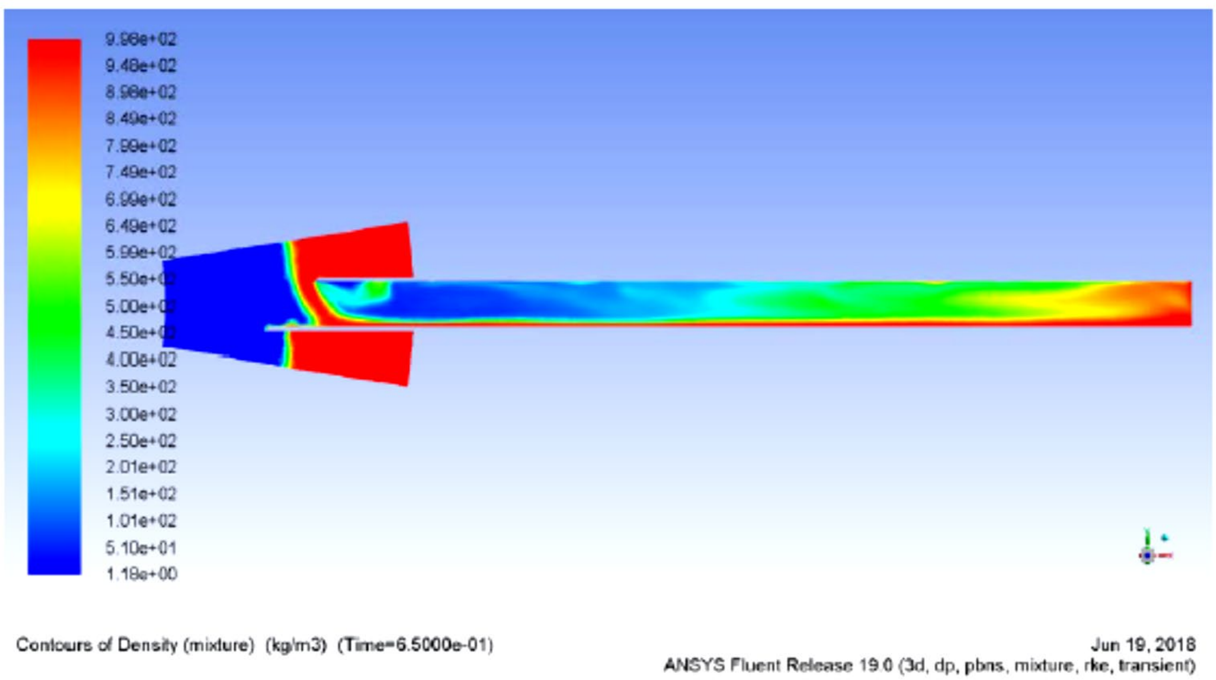

ANSYS fluent flow mix density (kilogram/cubic meter) CFD results of recirculation and energy recovery turbine

Source: Carnot Compression Inc.

Recirculation System – Recirculation and Energy Recovery Turbine

During testing it was established that accelerating the water to achieve the forces necessary to compress the emulsion of water and air required a significant amount of energy, and it became apparent that some of that energy would need to be recovered to help improve the efficiency of the system. A proposed solution was the recirculation and energy recovery turbine (RERT), a turbine that slowed the water exiting in the drain column to generate both shaft torque (to spin the rotor of a generator) and sufficient head (to return the water to the center of the compression drum). Carnot performed a literature review that led to nomographic-based designs for the turbine blades, which were also analyzed with CFD. Simulations suggested that recovery efficiencies of 85–95 percent were possible.

Heat Management

As with other aspects of the design process, engineering/mathematical modelling was employed as a first pass to study the impact of the heat of compression for 30 standard cubic feet per minute (SCFM) followed by CFD modelling. The results from these analyses suggested that about 750 watts (W) of heat would be lost naturally through the compression drum walls and the balance of 3,100 W would be left within the water, thereby necessitating the use of an external cooling loop for the water under the given design conditions (ambient temperature 300 kelvin [K] or the equivalent of 80°F [27°C] and 80 percent relative humidity [RH]). This work also resulted in the development of models that would allow the team to quickly calculate the heat transfer and power required to spin the compression drum based on the rotation speed and water-air temperature delta, further informing the design.

Water Management

The preliminary design included the use of a recirculation system to allow for heat rejection and reuse of the water used to compress air. The team needed to not only consider water quality from the feed water source but also address any water quality impacts that may result from the quality of the ambient air, given that the process is also effective for filtering air. For example, the high surface-area-to-volume ratio of the water/air emulsion provides a great way to transfer not only heat but also mass, such as suspended particulates and other constituent gases present in the ambient air (including the air itself).

The methods for preventing particulate matter (including microbes) from being entrained in the water was straightforward. Doing so was addressed first by way of an air filter; however, the more challenging aspect was addressing the dissolution of air and contaminant gases into the water during compression, the latter of which would be dependent of course on the location of the installation. Moreover, for installations in places where humidity is often high, the compression of ambient air would add some water to the balance' an example provided by the design team for the compressor operating at the target design conditions under 90 percent RH and 80° F (27°C) (300 K) suggested that a rate of 0.27 gallons of water per hour would be collected from compressing humid ambient air.

The impact of the dissolution of air into the water (and its impact on pH and other water quality indicators) was not addressed; however, since it was likely that there would be a need for purging the water from the system between cycles during testing, the focus was principally on the particulate filtration to avoid the accumulation of particulates within the system, which would impact operation and potentially harbor microbial growth.

Final Design – FD3 Prototype

As previously mentioned, the FD2 test bed served to provide preliminary engineering design data to assist with the final design for the FD3 prototype that would be deployed to the field site. The following sections review the results of additional testing performed on the sections covered by the FD2 testing as well as the additional elements of design needed to produce an alpha prototype.

Compression Tube Design

As a result of data regarding the diameter of the tubes and the impact of having a non-tapered open entry to the tubes, the design team elected to employ the use of V-shaped channels instead of tubing. Stacks of, first, V-shaped plates and, later, V-shaped blocks were set in place to delimit the compression channels within the drum. This change not only improved the performance but also added to modularity — allowing manufacturers to easily change the number of compression channels as needed. Other impacts the team noted about This design choice also resulted in fewer internal leak paths as well as a reduced number of parts needed for assembly and, consequently, reduced assembly time.

Recirculation System — Static Vane Return

As further testing was completed, the RERT system was found to have a negligible impact on the net power consumed by the compressor for the selected turbine design. The RERT was also noisy, complex, required frequent maintenance, was prone to failure, and added significant cost to the bill of materials, with two drives instead of one, a generator, and the need to oversize the compressor's main motor. Based on those cost and maintenance/reliability questions, it was preferable to switch from the RERT to a static vane return (SVR) concept.

The blue arrows in Figure 5 below illustrate the recirculating flow of the process water. The arrow at the top shows the water rotating, with the outer drum being captured by the stationary SVR to return to the center of the drum. The water is then mixed with incoming, uncompressed air, shown by the arrow pointing down. The air/water mixture flows outward through the compression tubes, shown by the bottom arrow. In the final step, shown by the upward arrow, the water builds up in the inner surface of the compressor drum until it is again captured by the SVR.

Figure 5: Static Vane Return Schematic

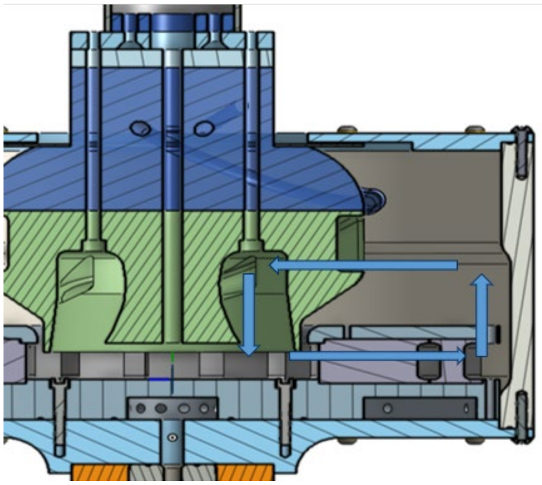

CAD assembly schematic of the compressor drum showing the water flow through the SVR

Source: Carnot Compression Inc.

The SVR would also collect water from the drain column at a high momentum and reintroduce it into the compression drum; the goal is that the water impinging on the compression channels would help contribute to the angular momentum of the drum, thereby helping to spin the compressor. While the RERT approach aimed at converting as much rotational energy as possible to electricity from the rotational momentum of the water, the SVR instead tries to conserve the rotational momentum in the water while returning it to the inlet of the compression element. The result was a significant reduction in system complexity, maintenance needs, and construction costs, with an increase in overall reliability.

Heat Management

Two pitot tubes were added into the compression drum to recoup a small fraction of the water in the drum, some of which would return via the SVR. The pitot tubes redirect this warmed water to their own radiators. The cooled water from the radiators then passes through a filter and is sent to the buffer tank before it is reinjected through the air inlet into the compression drum. Figure 6 shows the locations of the radiators, filter, and buffer tank.

Figure 6: Water and Heat Management Components

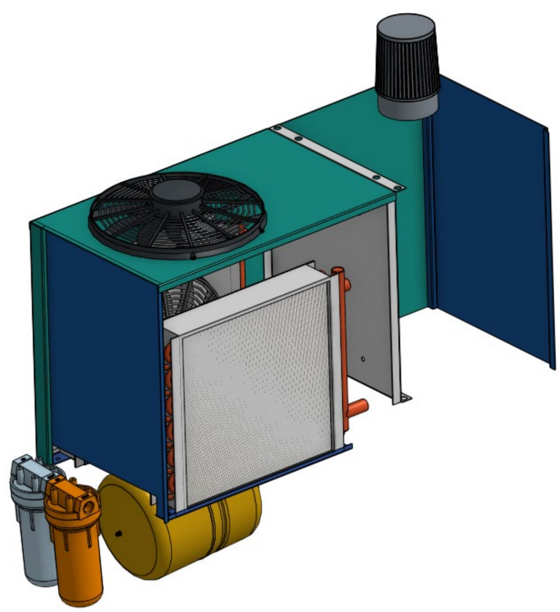

CAD assembly rendition of the water and heat management components

Source: Carnot Compression Inc.

Water Management

The buffer tank is necessary for the water that is added to the balance from the compressed air (noted as being 0.27 gallons per hour under high humidity). The buffer tank allows the system to dictate the water flow needed for cooling, in addition to the balance of water needed for optimal air compression in the compression drum.

Additionally, as previously mentioned in the Water Management subsection of the Preliminary Design – FD2 Test Bed and Six-tube Device section, the system would need to provide filtration for dissolved solids and gases. To do so, the fill system included a five-micron sediment filter for dissolved solids, a carbon filter for nonpolar organic compounds,[1] and a reverse osmosis filtration system for ionic compounds. The cooling loop also incorporated a 50-micron filter. As mentioned previously, the air inlet to the compressor made use of an air filter.

Data Acquisition System

GTI developed a data acquisition system to monitor the FD3 prototype for lab and field testing. The system included various sensors, including pressure, temperature, relative humidity, and metering for power consumption and mass flow. The sensors and meters were connected to a remotely accessible Campbell CR1000X, from which both GTI and Carnot could download data but which only GTI could program. This allowed the project team to fulfill the requirements for third-party monitoring of the system and gave Carnot the opportunity to actively monitor the system in parallel. The system was mounted on a separate skid and installed adjacent to the packaged compressor for lab and field testing. A detailed review of the monitoring system is provided in the Measurement Points and Data Acquisition System section of this report.

Chassis and Structural Elements

The final design included efforts to package all the compressor components as compactly as possible to minimize its footprint without impacting performance and safety. The final design for the packaged compressor employed a chassis that would be equipped with forklift pockets for ease of installation, adjustable feet for proper leveling, and a cage for the spinning compression drum for safety. The footprint of the packaged compressor would occupy a space of roughly 1.5 feet x 5.5 feet x 4 feet with the chassis supporting: the drive motor (Figure 7); the compression drum cage supporting the static elements of the system (the SVR), as shown in Figure 8; the data acquisition system's power metering enclosure and system programmable logic controller (PLC); the water management system; the cooling system (radiators and fans); the filtration system; the small air tank; and shielding panels.

Figure 7: Structural Element — Chassis Design

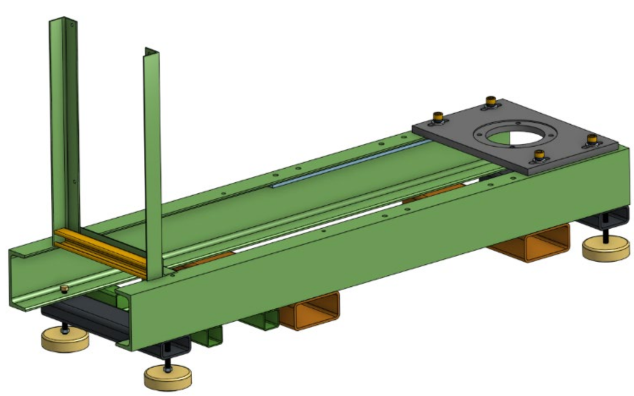

Computer-aided design assembly model of the chassis design

Source: Carnot Compression Inc.

[1] Activated carbon also adsorbs halogenated substances and lead, as well as other chemicals, and provides some additional sediment filtration.

Figure 8: Structural Element — Compression Drum Cage

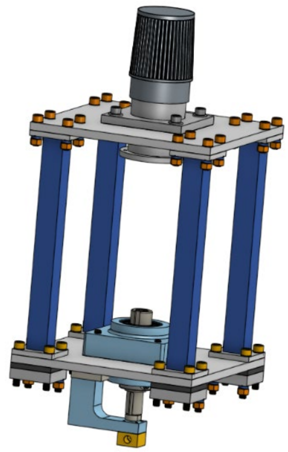

Computer-aided design assembly model of the compression drum cage

Source: Carnot Compression Inc.

Process Hazard Analysis

As part of the final design process, a process hazard analysis[2] was conducted to identify both the likelihood and the severity of potential hazards that would result from off-operating conditions. A thorough review was conducted of each hazard and the likelihood of occurrence to produce a risk ranking and to develop the appropriate safeguards to prevent injury to persons and/or damage to the FD3 prototype. Safeguards included thermal switches, physical measures (such as the compression drum cage), electrical safety devices such as breakers and manual disconnect, overtemperature alarms, and pressure relief valves.

Preliminary Testing and Final Design Parameters

Once the FD3 prototype had been manufactured, an initial round of testing was performed prior to delivery to the GTI lab to ensure proper operation and allow for any final design modifications. Major changes to the system were: slowing the drum from 3,600 RPM to 2,840 RPM to minimize spray and internal leakages; changing the compressor drum's flange to a fixed flange (Figure 9); blocking off one of the two pitot tubes; piping the radiators in series rather than parallel; changing the air filter model; rearranging buffer tank piping to the radiators; and removing the reverse osmosis system.

Additionally, the initial testing period was used to balance the spinning drum with the assistance of the subcontracted manufacturing company Kor-It. The balancing procedure was important, as it had identified that the old flange holding the compression drum shaft was not suitable for this application, having partially given way during the balancing procedure. Although the change to a fixed flange design reduced serviceability, it provided increased strength and durability to improve the safety of the device.

[2] Process hazard analysis is a study used to identify hazard scenarios for a process that could adversely affect people, property, or the environment. Scenarios examined include those that may result in fires, explosions, chemical spills, or release of toxic fumes or chemicals.

Figure 9: Compression Drum Shaft Flange Design Change

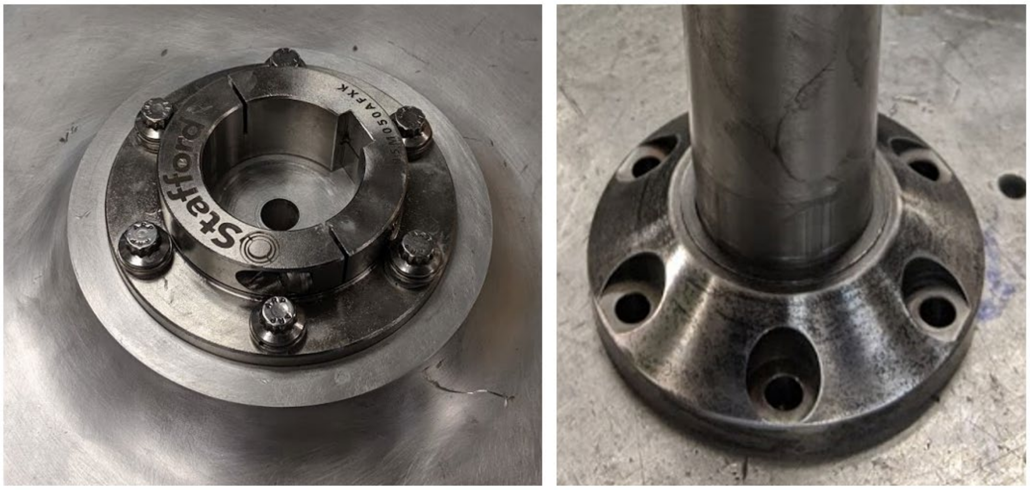

Design change of the compression drum shaft flange: initial flange on the left and updated flange on the right

Source: Carnot Compression Inc.

The initial runs showed that the modifications made to the internals of the FD3 prototype in addition to the slowing of the compression drum had reduced the output pressure of the system to 82 psig. Table 1 shows a summary of the progression of prototyping leading to the development of the FD3, along with the lessons learned from each iteration/test device.

Table 1: Summary of All Prototyping Progression

Prototype Name	Design Characteristics	Intent of Prototype Design Changes	Lessons Learned
1-g Taylor	15-ft vertical tube, one water jet emulsifier, static design	Demonstration of basic principle of the isothermal compression technology	Water velocity in the compression tubes must be higher than bubble rise velocity.
RoTaylor 1	Two tubes rotating compressor	Miniaturization and rotating compressor feasibility demonstrator	Visual proof of concept, pressure relationship to rotational velocity
RERT-Taylor 1	Two tubes rotating compressor, two channels recirculation turbine	Water recirculation and energy recovery demonstrator	68–74% torque recovery, first demonstrated use of castellated tube entries
FD1	800 tubes rotating compressor	Higher flowrates demonstrator and data gathering device	External recirculation systems require a booster pump and excess losses.

Prototype Name	Design Characteristics	Intent of Prototype Design Changes	Lessons Learned
RERT-Taylor 2	Two tubes rotating compressor, two channels recirculation turbine	Water recirculation and energy recovery improvements	Uses twin-bladed pitot that returns more than 80% of the input torque. Compression tube water seals have potential.
6-Tube tester	Six tubes compressor, easily replaceable tubes	Benchtop device for tube geometry testing and CFD simulations validation	Device allowed a tube selection for the CEC* test unit and demonstrated that CFD was not able to accurately model compression tubes.
FD2	Modular evolution of FD1	Internally recirculating compressor, test bench for various components and technological options at higher air flows	Larger compression tubes/ channels are better; both RERT and SVR work as intended; significant improvements in device manufacturability, efficiency, and reliability.

*CEC = California Energy Commission
Source: Carnot Compression Inc.

Table 2 shows the finalized specifications for the FD3 system before it was sent to the GTI laboratory test site. This data was not collected with the GTI monitoring system.

Table 2: Final Pre-testing FD3 Specifications

Parameter Name	Design Value
*Air Production**	5–7 ACFM** at 82 psig
Max. Delivery Pressure	85 psig
*Power Consumption**	17–23 HP (12.7–17.2 kW)
Motor Nameplate	15 HP 3-phase single-speed motor
	208–240/480 V
	1750 RPM
Envelope/Footprint	1.5 ft x 5.5 ft x 4 ft
Compressor Drum Dimensions	17” OD (outside diameter) x 15” H
*Weight**	Approximately 750 lbs
Drum Rotation Speed	2840 RPM
Air Receiving Tank Capacity	5 gallons

Parameter Name	Design Value
Operating Water Volume	6–7 gallons total
	3 gallons total in compression drum
Water Drainage Rates	During Operation: Variable up to 1.5 gallons/hour
	Full Drain: 6–7 gallons total
	Compression Drum Drain Only: 3 gallons total
*Operating Water Temperature**	Up to 50°F over ambient
*Noise Level**	85 to 90 dB***
Vibration Level	Not measured, but generally very low amplitude with some transient low-frequency modes of low-to-moderate amplitude.

* estimated values
** ACFM = actual cubic feet per minute
*** decibels
Source: Carnot Compression Inc.

Engineering Design Changes During Testing

Further modifications occurred during the lab-testing phase and a final change was implemented during the field-testing phase before freezing the design. Those changes are included and detailed in the following paragraphs, and some are covered in more detail in the Commissioning and Lessons Learned subsection of the Field Testing Results section of this report.

The cooling loop was modified in two steps: first, the 12- and 24-volt (v) fans were replaced by 120-volt fans for simpler wiring and more efficient cooling, and second, the entire on-board cooling was replaced by an external module to release heat outside of rather than in the same room as the FD3. This switch to an external module also allowed use of different cooling means, such as the initial water/air approach, a water/water heat exchanger, an open loop, and a heat recovery system. The external module used during testing was consistent with the original prototype’s water/air approach.

Vibration dampeners were added to the mounting system of the controls cabinet and the controls themselves went from analog switches to a PLC, as it was found that the switches were too sensitive to the occasional vibrations and caused random shutoffs.

The power elements (starter and relay) were moved during the field-testing phase (all other modifications were implemented during the lab testing) to a box separate from the controls cabinet, as heat buildup inside the cabinet was detrimental to the PLC. A wiring error and repeated running of the FD3 at power levels greater than its motor nameplate value significantly taxed the 15-HP motor and its soft starter. The motor was subsequently replaced by a 20-HP motor and the soft-starter by a three-phase relay (the change was done without increasing the power usage settings of the FD3). Figure 10 shows the FD3 in the lab setting.

Figure 10: FD3 Installed at GTI Laboratory

Carnot FD3 unit for lab testing

Source: Carnot Compression Inc.

Lab and Field Testing

The main objectives for both lab and field testing were to 1) evaluate the performance of Carnot's prototype isothermal compressor against benchmark values and 2) to test for any environmental impacts resulting from the prototype's operation, specifically wastewater composition, sound intensity, and vibration. Performance metrics were collected for steady-state operation in the lab and on a compression cycle basis in the field. Environmental testing was conducted only in the lab. The following sections present the data acquisition system, calculations, and test procedures used to collect and analyze the data for the evaluation of the system's performance and environmental impacts.

Measurement Points and Data Acquisition System

The only required points of measurements necessary to calculate the performance metrics were power consumption, mass flow, and the inlet/outlet state variables (pressure and temperature). The sound, vibration, and water testing were not continuously monitored, and the equipment required to carry out the testing is covered later in their respective protocol summaries.

Starting Data Acquisition System Configuration

The points of measurement began with ambient temperature and relative humidity, which provided data on incoming air conditions at the standard air inlet point to the compressor package. The temperature and relative humidity were measured with one Pt1000 resistive temperature device (RTD). Figure 11 and Figure 12 illustrate the specifics of the configuration.

Within the compressor package there were two WattNode power meters for measuring 1) the electricity consumption of the compressor motor (E1) and 2) the electricity consumption of the ancillary systems, such as valves, water sump pump, control system, and fans (E2). The return for the water loop also included a type T thermocouple for measuring water temperature (T4).

A coriolis mass flow meter (F1) was plumbed in line to measure compressed air flow. A refrigerated dryer with a zero-loss condensate drain[3] (D1) was also added, partly through testing to minimize the impact of condensation on the flow measurements. The dryer was also metered but no usable data was obtained, and, in any case, dryers are not typically part of a packaged compressor. The dryer power consumption was not included in the calculation of the efficiency or specific power as a result.

As previously mentioned, the monitoring skid plumbing includes tees for 1) a pressure transducer (P1), which was positioned upstream of the dryer for measuring delivery pressure; 2) a sheathed type T thermocouple (T3) for measuring delivered air temperature (also upstream of the dryer); and 3) a dew-point temperature sensor (Td1) for measuring the relative humidity downstream of the refrigerated dryer. It should be noted that the mass flow meter (F1) also provided temperature data via an RTD; however, the RTD was not directly exposed to the compressed air.

Changes to Data Acquisition System Configuration

Field testing required 1) changing the flow meter,[4] 2) adding a dew point temperature sensor, and 3) moving the outlet temperature thermocouple and outlet pressure transducer to the air receiving tank as opposed to the compressed air discharge outlet. The changes may be evidenced by comparing Figure 11 and Figure 12.

Figure 11: Lab Measurement Point Schematic

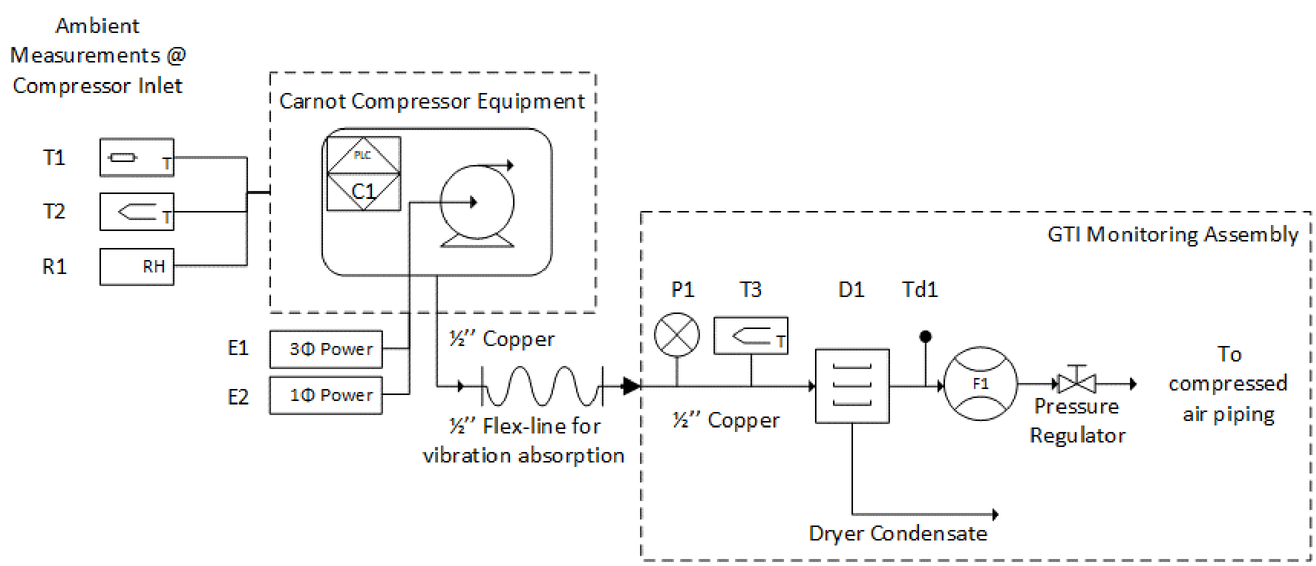

Flow schematic for lab measurement components

Source: Gas Technology Institute

[3] Zero-loss is in regard to the pressure: some air is likely lost during the purging of the condensate from drying the compressed air.

[4] Several flow meters were used throughout the course of the project. All three are listed in Table 3. The coriolis flow meter was used for most of the lab testing. The coriolis flow meter was briefly supplemented by a thermal dispersion meter during the lab testing and ultimately replaced by a laminar flow element differential pressure mass flow meter in the field.

Figure 12: Field Measurement Point Schematic

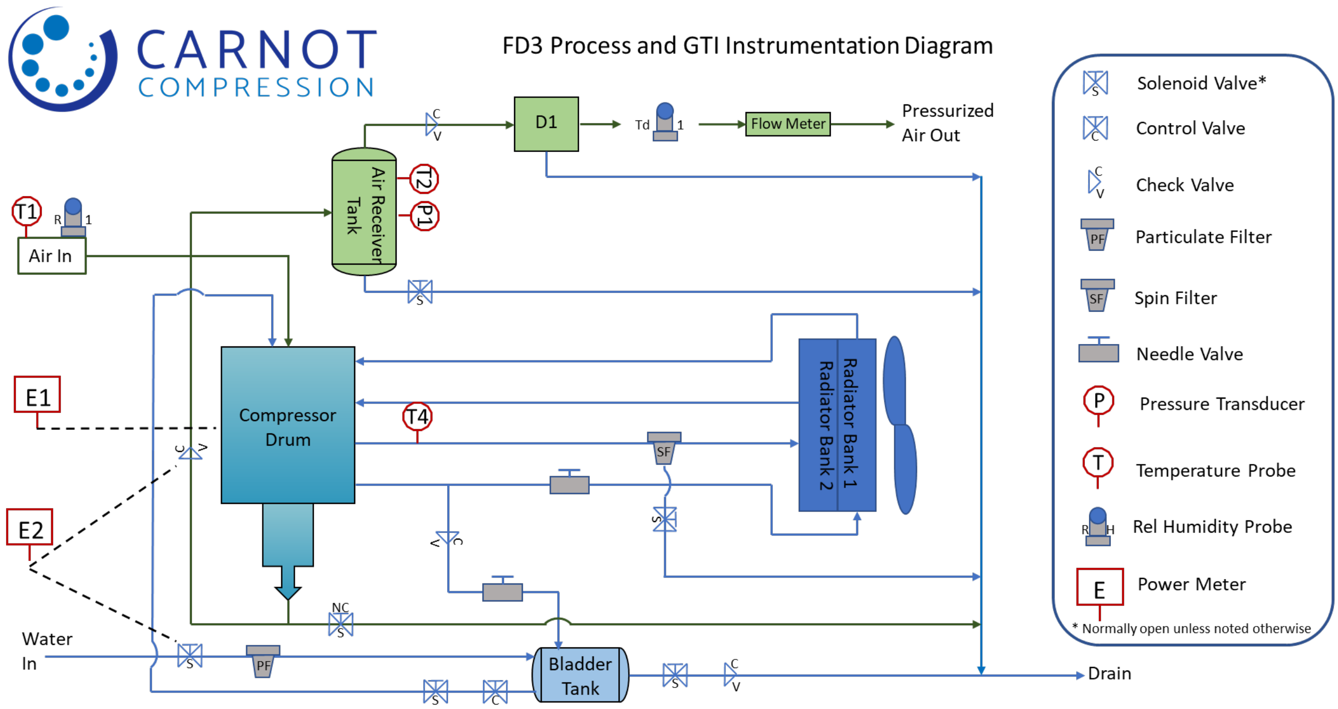

Flow diagram of major system components of the FD3 process and GTI instrumentation

Source: Carnot Compression Inc.

Sensors

Table 3 summarizes the measurement points respective sensors. The I.D. column of the table refers to the measurement point schematic pictured in Figure 11 and Figure 12.

Table 3: Measurement Points and Equipment

Parameter	I.D.	Model Numbers	Accuracy
Ambient Temperature	T1	Vaisala HMP110	± 0.36°F (0.2°C) (32–104°F)
Ambient Relative Humidity	R1	Vaisala HMP110	± 1.5% RH (0–90% RH)
Water Loop Temperature	T2	ProSense THMT-P06-01 Type T Thermocouple	± 1.8°F (1°C)
Compressor Motor Power	E1	RWNB-3D-240-P Revenue Grade WattNode Pulse 3x 50A ACTL-0750-050 Opt. C.06 Current Transformers	± 0.5% reading

Parameter	I.D.	Model Numbers	Accuracy
Ancillary Power	E2	RWNB-3Y-208-P WattNode Power Meter	± 0.5% reading
		1x 20A ACTL-0750-020 Opt. C.06 Current Transformers	
Compressed Air Flow Rate	F1	Emerson Micro Motion R025S with Micro Motion 2700 Integral Mount Transmitter	Mass Flow: ± 0.75% Temp: ± 0.5%
		Omega Model FMA1844-A	Mass Flow: ± 1.5%
		Alicat M-100	Mass Flow: ± 0.8% Pressure: ± 0.5% Temperature: ± 1.35°F (0.75°C)
Delivered Air Temperature	T3	ProSense THMT-P06-01 Type T Thermocouple	± 1.8°F (1°C)
Delivered Air Pressure	P1	ProSense SPTD25-20-0200H	<± 0.5% reading
Dew Point Temperature	Td1	Vaisala DMT143	± 3.6°F (-76–86°F) [2°C (-60-30°C)]

Source: GTI

Performance Testing Summary

Laboratory Performance Testing

Performance lab testing focused on measuring the steady-state energy consumption, state variables, and compressed air flow rate to provide the required data for comparing the prototype's performance against industry benchmarks by way of isentropic efficiency and specific power. The testing procedure was modeled in part after International Standardization Organization standard 1217 Displacement Compressors — Acceptance Tests. Comparable compressors were chosen as benchmarks in base of the characteristics reported on their Compressed Air & Gas Institute (CAGI) datasheets for Rated Capacity at Full Load Operating Pressure (Item 3) and Full Load Operating Pressure (Item 4). The resulting specific power and isentropic efficiency from the FD3 prototype's steady-state data was compared against the reported Specific Package Input Power at Rated Capacity and Full Load Operating Pressure (Item 12) and Isentropic Efficiency (Item 13) of the benchmark's CAGI datasheets. The steps for calculating the isentropic efficiency and specific power from lab and field data are covered in the Calculation Methods section of this report.

Additionally, the initial test plan called for varying lengths of testing periods, noted as short- and long-interval tests. Early testing stages involved short-interval periods of eight 15-minute and four 30-minute tests. Long-interval testing commenced thereafter, including multiple days of six 1-hour interval tests, two 4-hour tests, and one 8-hour test. Early short-interval tests were meant to serve as troubleshooting opportunities. Each successive test culminated in long (8-hour) testing to prepare the unit for field deployment.

Field Performance Testing

The laboratory settings allowed for testing the prototype under steady-state conditions; however, the actual use of compressors depended on the demand for compressed air. As such, the compressor was connected to the host site's compressed air system and operated as needed with the regulator supply compressed air between approximately 98 psig and approximately 113 psig.

For this portion of the project, the data collected was parsed by "tank fill" and "tank drain" events. The events were delineated by the rise in pressure of the air receiving tank ("tank fill") followed by the drop in air receiving tank pressure caused by the opening of the regulator to the compressed air system ("tank drain"). For data where only state variables (pressure and temperature) were available, only the "tank fill" parsed data was used to calculate the mass flow rate, as detailed by the state variables approach outlined in the Calculation Methods section. For periods where the Alicat mass flow meter was available, both the "tank fill" data and the "tank drain" data were used, with the state variables approach used to calculate the mass flow rate for the "tank fill" event (as the mass flow meter would not register flow until the regulator opened) and the directly measured mass flow data from the meter used for the "tank drain" events. In either situation, the calculated and/or measured mass flow was averaged over the given interval and used to calculate the isentropic efficiency and specific power for the compressor, as detailed in the Calculation Methods section.

Environmental Test Procedures Summary

Environmental testing for sound and vibration was conducted only at the Reno facilities during the lab testing phase and not at the field site. Water testing was conducted only at the Davis laboratory and not the Reno lab test site. The following sections cover the procedure for each of the environmental test categories of sound, vibration, and water composition.

Sound Intensity Measurements

Summary

Sound intensity tests were performed with the compressor on the ground (concrete slab) and then on a dedicated stand at the Reno testing site, with access panels fully installed and fastened. The sound measurement procedure for Carnot Compression's FD3 prototype was modeled after International Standardization Organization 2151, Acoustics — Noise Test Code for Compressors and Vacuum Pumps, Engineering Method (Grade 2), based on suggestions from CAGI. Initially the project team had planned to use the National Institute for Occupational Safety and Health (NIOSH) Sound Level Meter app to measure loudness in decibels A (dBA), but GTI supplied a handheld sound meter for use in testing.

Procedure

The following procedure was used to measure the FD3 sound levels. The measurement points for this procedure are indicated on the FD3 compressor in Figure 13.

1. Open/use the NIOSH Sound Level Meter app or handheld sound meter using dBA.
2. Ensure the unit is turned off.
3. Begin from the corner near motor (marked 1 in the photo below) and work around the compressor counterclockwise, writing down the values at each numbered location. Each measurement should be taken 1 meter (m) (3.2 feet) away from the compressor, with the microphone end of the phone facing the compressor while the phone remains horizontal, 1.6 m (5.3 ft) above the ground and about an arm's length away from the body. Consult the noise info tab in the NIOSH phone app to determine the appropriate duration for each measurement point and the proper procedure if needed.
4. Repeat step 4 with the compressor running at full load.

Figure 13: Sound Measurement Location References

FD3 sound testing with key referenced locations

Source: Carnot Compression Inc.

Vibration Measurement Procedure

Summary

Vibration measurements were taken with an Omega HHVB82 handheld accelerometer, which is capable of recording peak and root mean square values for acceleration and velocity along Cartesian coordinate axes noted as vertical (z-axis), longitudinal (x- or y-axis), and lateral (x- or y-axis). No other instruments were required.

Velocity measurements were compared to values obtained from the 1999 ASHRAE Applications Handbook section on vibration isolation and control, shown in Figure 14. For Good or better measurements, no isolation was needed. Scores of Fair and Slightly Rough may indicate potential problems, while Rough and Very Rough indicate potentially serious issues. While these guidelines are intended as a means for evaluating unwanted noise and vibration from HVAC equipment installed inside, adjacent to, or on top of buildings, they may also be useful for providing a basis of comparison for the prototype compressor and where it may be installed.

According to the material in this section of the ASHRAE handbook, the readings should be taken when the equipment is installed directly on a concrete slab.

Figure 14: Equipment Vibration Severity Root Mean Square Velocity Scale

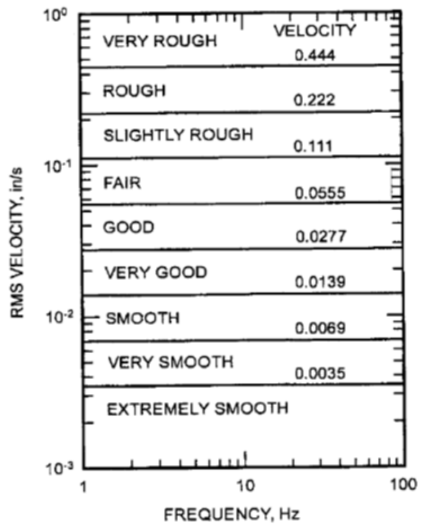

Equipment vibration severity for vibration measured on equipment structure or bearing

Source: ASHRAE

Procedure

The procedure involved ensuring that the compressor was placed on a concrete slab. While the compressor was running at full load, an accelerometer was affixed to the compressor and collected approximately 30 seconds of data for each location of interest. The locations are marked on Figure 15 and are described in Table 4.

Figure 15: Vibration Testing Locations

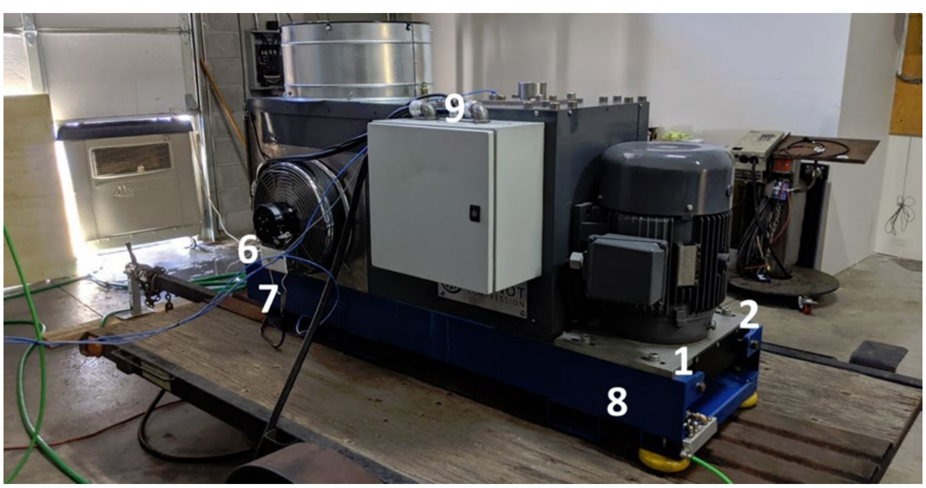

FD3 system on test bed with some key vibration testing locations noted

Source: Carnot Compression Inc.

Table 4: Vibration Testing Location Descriptions

Location ID	Location
1	Top of skid, next to motor, same side of gray enclosure
2	Top of skid, next to motor, opposite side of gray enclosure
3	Side of skid, next to motor (not pictured and directly opposite position 8)
4	Side of skid, next to fans (not pictured and directly opposite position 7)
5	Top of skid, next to fans, opposite side of gray enclosure (not pictured)
6	Top of skid, next to fans, same side of gray enclosure (not pictured)
7	Side of skid next to fans
8	Side of skid next to motor
9	Center of the top of the gray (power metering) enclosure

Source: GTI

Water Testing

Summary

Water sample testing was performed by Test America for the samples collected by the project team. The water samples were collected at the Davis lab using the feed water to the compressor and the discharge from the compressor to evaluate whether the compressor's wastewater significantly impacted water quality. Measurements resulted in data on dissolved metals, dissolved anions, pH, total organic carbon, conductivity, total dissolved solids, and hardness. Testing included scanning electron microscopy with energy dispersive X-ray spectrascopy (for elements present), x-ray diffraction (to identify any crystalline material), and analysis for carbon, hydrogen, nitrogen, and sulfur (to differentiate if any organics are present).

Procedure

Three water samples were collected for both the feed and the discharge water using the provided collection containers in the volumes prescribed by the testing agency. Container 1 consisted of a 125-millileter (ml) plastic bottle preserved with nitric acid for the metals. Container 2 was a 40-ml glass vial preserved with sulfuric acid for the organic carbon analysis. Container 3 was a 500-ml plastic bottle with no chemical reagent. The samples were packaged in a cooler with ice packs and shipped overnight to the testing facility. The chain of custody record was then completed. Figure 16 shows the chain of custody record required for the samples.

Figure 16: Water Sampling Chain of Custody Record for Davis Lab Testing

Chicago
2417 Bond Street

University Park, IL 60484
phone 708.534.5200 fax 708.534.5363

Chain of Custody Record

TestAmerica
THE LEADER IN ENVIRONMENTAL TESTING

TestAmerica Laboratories, Inc.

Client Contact	Project Manager: Karen Crippen	Site Contact: Eric Brown		COC No: 1
Gas Technology Institute	Tel/Fax: (847) 768-0604 / (847) 768-0970	Lab Contact: Eric Brown	Carrier: (T/A pickup)	___1___ of ___1___ COCs
1700 Mount Prospect Road	**Analysis Turnaround Time**			Job No.
Des Plaines, IL 60018-1804	Calendar (C) or ~~Work Days (W)~~ __Calendar__			
(847) 768-0729 Phone	TAT if different from Below ________			
(847) 768-0970 FAX	☐ ~~2 weeks~~			SDG No.
Project Name: "**22150.4.01 Carnot Compressor Testing**"	■ 1 week			
Site: GTI - Des Plaines	☐ ~~2 days~~			
P.O. #: **VT00079693**	☐ ~~1 day~~			

Sample Identification	Sample Date	Sample Time	Sample Type	Matrix	# of Cont.	Filtered Sample	Metals Analysis ICP/MS (200.8)	pH	Total Organic Carbon (9060A)	Conductivity	Hardness	IC anions	Total Dissolved solids	Sample Specific Notes:
202079-003, Davis Inlet Water			Aqueous	Water	One	NO	X	X	X	X	X	X	X	Please analyze dissolved metals and anions
202079-004, Davis Discharge Water			Aqueous	Water	One	NO	X	X	X	X	X	X	X	Please analyze dissolved metals and anions

Preservation Used: 1= Ice, 2= HCl; 3= H2SO4; 4=HNO3; 5=NaOH; 6= Other ___NONE___4_____

Possible Hazard Identification
☐ *Non-Hazard* ☐ *Flammable* ■ *Skin Irritant* *Poison B* ☐ *Unknown* ☐

Sample Disposal (A fee may be assessed if samples are retained longer than 1 month)
☐ *Return To Client* ■ *Disposal By Lab* ☐ *Archive For __________ Months*

Special Instructions/QC Requirements & Comments: **Anions- Fluoride, Chloride, Nitrate, Sulfate,** Metals- As, Se, Cd, Pb, Hg, Ba, Ag, Cr, Mn, Zn, Ni, Cu, Fe, K, Na, Mg, & Ca

Chain of custody record for water sample testing procedure

Source: TestAmerica Laboratories Inc.

Calculation Methods

Both the isentropic efficiency and the specific power are available on the CAGI data sheets. The following sections begin with a review of the calculation methods for measuring these performance metrics used to compare the prototype isothermal compressor against the selected benchmarks.

Isentropic (reversible adiabatic) efficiency is a commonly used metric by which the prototype may be compared against benchmark compressors. Effective March 10, 2020, the U.S. Department of Energy final rulings for compressor efficiency standards have established isentropic efficiency as a standard for compliance under the Energy Policy and Conservation Act of 1975 (U.S. Department of Energy, 2022); therefore, isentropic efficiency was used as a basis for comparison against industry benchmarks. Additionally, isentropic efficiency is a better metric for comparing energy consumption than the specific power since isentropic efficiency accounts for the compression ratio (as detailed later in this section). Regardless, despite specific power being useful only for comparing compressors operating at the same delivery pressure, the project team decided it would be useful to include this metric in the analysis, as specific power is commonly available in the specifications for compressors.

Lastly, the project team decided that it would be useful to model the data as a polytropic process[5] and employ the polytropic work equation for calculating the theoretical work/efficiency, for two reasons: 1) setting the polytropic index to 1.4 yields isentropic work and 2) by calculating the actual polytropic index (as opposed to setting it to 1.4), the project team may also see how closely isothermal the compression was since isothermal processes have a polytropic index of 1.

Mass Flow Rate — State Variable Approach

Due to the metering difficulties described in the Testing Barriers section, most of the mass flow data from the field testing was obtained using the ideal gas law equation of state. Using the ideal gas law and the state variables (pressure and temperature) of the compressed air in the receiving tank, which was of a known volume, it was possible to approximate the average flow rate for a given compression event. The mass flow rate obtained with the "state variables approach" was later compared against directly measured mass flow for validation, which is covered in detail in the State Variable Approach Validity Analysis section.

Testing Sites

GTI Facility — Davis, California

Testing for the FD3 prototype was planned for the GTI facilities in Davis. A process hazard analysis was conducted to ensure that the unit would be safely run in the lab's environmental chamber, which could provide tightly controlled conditions for testing. The prototype was

[5] A thermodynamic process relating a gas state's pressure and volume through incorporating the polytropic index.

installed in March 2020 (Figure 17), but COVID-19 pandemic lockdowns delayed testing and ultimately the team relocated testing to Carnot's facility in Reno, Nevada, in July 2020.

Figure 17: FD3 Compressor Installed in Davis Lab Environmental Chamber

FD3 hosted for testing inside GTI's Davis, California, lab

Source: GTI

Carnot Facility — Reno, Nevada

Carnot maintains an office and shop facility in Reno, Nevada. The lab testing of the FD3 took place at this location, under constant monitoring by the data acquisition system communicating its data to GTI (Figure 18).

Figure 18: Carnot Facilities in Reno, Nevada, During FD3 Lab Testing

FD3 testing at the Reno facility: (left) one of the numerous tests run and (right) another test run with a condensing unit

Source: Carnot Compressor Inc.

Litton Engineering Field Site

The field testing of the FD3 took place at Litton Engineering Laboratories in Grass Valley, California. The prototype was placed in the shed housing its backup compressor from late February to November 2021. It was plumbed into Litton's existing compressed air system, which supplies compressed air to its machine shops, just upstream of its collection tank and in parallel with both its primary rotary screw compressor and its backup piston compressor. The FD3 was programmed to operate from 7:00 a.m. to 5:00 p.m., weekdays only, and was expected to operate in tandem with the primary compressor. The FD3 prototype supplied compressed air to Litton's compressed air system for pressures between 98 and 113 psig.

CHAPTER 3: Project Results

Lab Testing Results

Performance Results

The initial results of lab testing presented here were collected for a short, approximately 15-minute run in which little condensation was likely produced. The data was collected before any electrical issues had manifested at the facility. The data is the best representation of the unit's capacity during lab testing, as the capacity was later impacted by troubleshooting as well as design changes aimed at further developing the technology and preparing the unit for field testing. These impacts are covered in the Testing Barriers section of this chapter.

The data from the initial lab testing on July 13, 2020, suggested that the prototype was capable of providing approximately 8.8 actual cubic feet per minute (ACFM), inlet at an operating pressure of approximately 78.7 psig; however, this was not consistently reproducible during lab testing. This data point is shown in Table 5 in comparison to the design target and the selected benchmarks for standard rotary screw compressors. Table 6 provides additional information on the test results.

Table 5: Benchmark Comparison

	Benchmark No. 1	Benchmark No. 2	Benchmark No. 3	Carnot Target (Commercial)	Carnot 7/13/2020
Make/Model	Sullivan Palatek/20D	Atlas Copco/ GA37-125	Atlas Copco/ GA200VSD-125	Carnot Compression/TBD	Carnot Compression/FD3
Type	air-cooled, single-stage, oil-injected, screw	air-cooled, single-stage, oil-injected, screw	water-cooled, single-stage, oil-injected, screw	n/a	water-cooled, single-stage, isothermal, centrifugal
ACFM	78	229	1241	30-1000+	8.77
Operating Pressure	125	125	125	100-125	78.7
kW/100ACFM	24.8	19.7	18.0	18.6-24.4	204
Isentropic Efficiency	43.9%	55.38%	60.6%	40.8-58.7%	4.09%

Source: GTI

Table 6: Performance Data Summary

	Average	RMSD*	Uncertainty/Error
Power Consumption, kW	17.33	± 1.4	± 0.086
Delivery Pressure, psig	78.7	± 0.35	± 1

	Average	RMSD*	Uncertainty/Error
Mass Flow Rate, kilogram/min and pound mass/min	0.249 / 0.550	± 0.0482 / 0.106	± 0.000421 / 0.000929
ACFM @ Inlet Conditions	8.77	± 1.69	± 0.94
Ambient Air Temperature	76.4	± 1.09	± 1.8
Compressed Air Temperature	76.3	± 0.670	± 1.8

* Root mean square deviation
Source: GTI

Environmental Test Results

Sound Intensity Testing Results

The results in Table 7 and Table 8 summarize the sound intensity measurements for the FD3 compressor and the condenser unit used for heat rejection. The compressor sound intensity measurements were taken when the compressor was both on a stand and directly on the concrete slab floor of the facility. The background noise was included and was predominantly from the condenser/heat rejection unit, measured at given locations around the compressor. Additional single-point sound measurements were taken for the condenser and dryer in operation for comparison. The picture from the procedure for the given locations was copied in after the tables for convenience (see Figure 19).

Table 7: Sound Intensity Measurements (dBA)

Location	Compressor on Stand	Compressor on Slab	Background Noise
1	79.8	79.5	59.2
2	78.3	79.7	64.1
3	78.9	79.2	56.2
4	78.2	79.4	57.8
5	78.7	79.0	54.1
6	77.97	78.5	57.1
7	79.1	80.5	53.6
8	78.3	79.7	56.6

Source: GTI

Table 8: Cooling Unit and Dryer Sound Intensity Measurements (dBA)

Equipment Status	Stopped	Running
Condenser	43	60
Dryer	39	56

Source: GTI

Figure 19: Sound Intensity Location References

FD3 model with key referenced locations for sound intensity testing

Source: Carnot Compression Inc.

Vibration Testing Results

Referring to Figure 11, the data in the following tables suggests that the unit will likely need to consider vibration isolation for installation on concrete slabs, as is common with many types of similar equipment or appliances. Testing was performed with the access panels of the compressor fully fastened and the compressor operating both on its test stand (Table 9 and Figure 20) as well as directly on the ground (Table 10).

Table 9: Vibration Velocity Results — Stand Resting Position

Location	Vertical [in/s]			Lateral [in/s]			Longitudinal [in/s]		
	mean	*max*	*min*	*mean*	*max*	*min*	*mean*	*max*	*min*
1	0.315	0.374	0.22	0.618	0.807	0.429	0.28	0.346	0.197
2	0.323	0.433	0.177	0.642	0.85	0.232	0.22	0.276	0.146
5	0.323	0.512	0.26	0.453	0.598	0.335	0.283	0.327	0.154
6	0.406	0.575	0.213	0.496	0.618	0.398	0.185	0.244	0.13
9	0.138	0.217	0.098	-	-	-	-	-	-

Source: GTI

Table 10: Vibration Velocity Results — Ground Resting Position

Location	Vertical [in/s]			Lateral [in/s]			Longitudinal [in/s]		
	mean	*max*	*min*	*mean*	*max*	*min*	*mean*	*max*	*min*
1	0.291	0.319	0.213	0.52	0.642	0.295	0.272	0.319	0.213
2	0.346	0.413	0.217	0.594	0.657	0.287	0.213	0.28	0.138
5	0.402	0.48	0.311	0.429	0.516	0.291	0.28	0.315	0.15

Location	Vertical [in/s]			Lateral [in/s]			Longitudinal [in/s]		
	mean	*max*	*min*	*mean*	*max*	*min*	*mean*	*max*	*min*
6	0.441	0.567	0.252	0.445	0.516	0.315	0.181	0.291	0.134
9	0.142	0.197	0.098	-	-	-	-	-	-

Source: GTI

Figure 20: Vibration Testing Locations

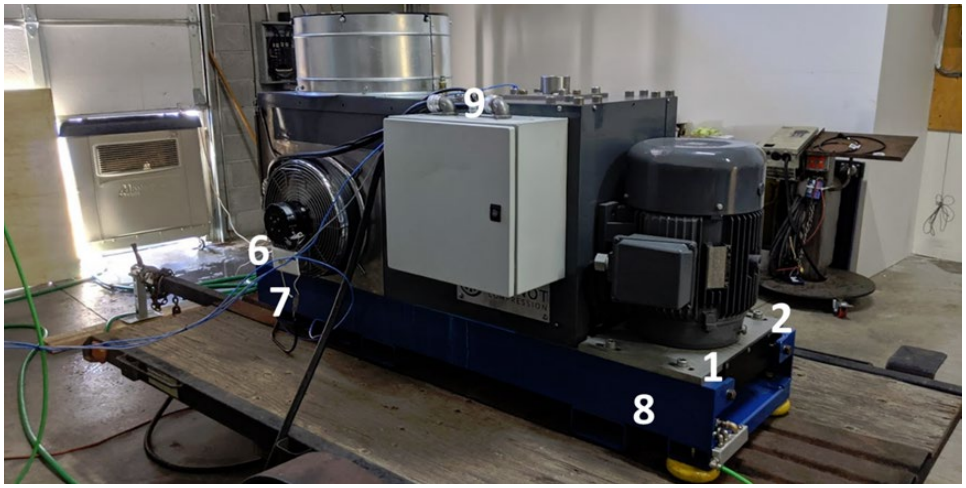

Key locations on FD3 for vibration testing

Source: Carnot Compression Inc.

Water Testing Results

The increases and decreases in the concentration of various metals between the feed water and the discharge water results suggest that some leaching and scale formation occurred within the prototype during operation (Table 11). For example, an increase in lead may be from newly brazed[6] components and an increase in iron (as well as other components present in stainless steel) may be from machined components in contact with the cooling water. There was also a notable decrease in calcium and magnesium, which supports the suggestion of scale formation. It may be useful to test the unit again after various lengths of run-time, to examine any changes over extended use. These results may also be used to inform future materials selection for the commercialized product.

Table 11: Water Testing Results

Measurement	Unit	Feed Water	Discharge	Notes
Arsenic	µg/L*	2.21	2.36	Increase
Barium	µg/L	212	4.90	Decrease
Cadmium	µg/L	ND	ND	Not Detected
Calcium	µg/L	62000	1700	Decrease

[6] Braze: The forming, fixing, or joining by soldering of an alloy of copper and zinc at a high temperature.

Measurement	Unit	Feed Water	Discharge	Notes
Chromium	µg/L	5.68	76.4	Increase
Copper	µg/L	89.7	1040	Increase
Iron	µg/L	ND	3270	Increase
Lead	µg/L	0.658	32.9	Increase
Magnesium	µg/L	130000	1490	Decrease
Manganese	µg/L	11.4	25.0	Increase
Nickel	µg/L	ND	421	Increase
Potassium	µg/L	1650	1800	Increase
Selenium	µg/L	37.9	37.8	Decrease
Silver	µg/L	ND	ND	Not Detected
Sodium	µg/L	117000	157000	Increase
Zinc	µg/L	38.4	99.2	Increase
Mercury	mg/L	ND	ND	Not Detected
Hardness as calcium carbonate	mg/L**	691	10.4	Decrease
Chloride	mg/L	115	110	Decrease
Fluoride	mg/L	0.223	0.528	Increase
Nitrate as N	mg/L	11.6	11.4	Decrease
Sulfate	mg/L	122	120	Decrease
Total Organic Carbon - Duplicates	mg/L	1.34	3.16	Increase
Specific Conductance (25C)	umho/cm***	1590	1760	Increase
Total Dissolved Solids	mg/L	1020	1130	Increase
pH	SU****	7.8	8.4	Increase

* micrograms per liter
** milligrams per liter
*** micromhos per centimeter
**** standard unit

Source: GTI

Testing Barriers

COVID-19 Impacts

As previously mentioned in the Testing Sites section of Chapter 2, the prototype was installed at a GTI testing facility in March 2020 but, due to COVID restrictions, the project team requested it be moved back to the Carnot facility in Reno, Nevada. The prototype arrived in Reno in July 2020 for supervised lab testing. Additional COVID-19 impacts were felt in the form of supply-chain disruptions as the project moved forward, such as extended lead times for the replacement flow meter and replacements for damaged thermocouples.

Low Flow and In-line Condensation

During initial lab tests, the project team suspected that the coriolis flow meter (Emerson) was not measuring mass flow reliably at the target delivery pressure (100-125–psig) due to low and unstable readings at 90 psig. It was suggested that condensation within the coriolis flow meter tubes, interference, incorrect wiring, or equipment damage was the root cause of unreliable flow values. From the compressor's arrival in July 2020 to August 2020, the project team explored potential issues. After verifying wiring connections, taking further observations (such as in-line condensation), and troubleshooting under the guidance of the manufacturer, it was determined that the flow meter parameters were in range and that the wiring was installed correctly. The manufacturer's technicians suggested that, at the target pressures, the flow may be below the mass flow rate cutoff of 1.08 grams per second (g/s) or 0.00238 pound mass per second (lbm/s) (approximately 1.9 SCFM) at higher delivery operating pressures and that, additionally, condensation within the testing skid was likely affecting measurements and causing offsets when the unit was not producing any air. Field measurements for the final design showed the flow rate at approximately 0.3 g/s.

At lower pressures and for short runs, the monitoring skid was able to register flows of approximately 6 ACFM, inlet at 70 psig. However, during longer periods of operation, flow measurements became unstable and deviated, likely due to the previously mentioned condensation. Also, additional support for condensation was seen with the observations for "no flow" conditions (for example, inlet and outlet of skid valved off) wherein the meter showed an offset of approximately 3–4 SCFM until the skid was tilted to release collected condensation (see Figure 21). Any condensation within a coriolis meter will cause offsets because the added mass adversely affects the meter's operating principle.[7]

[7] Coriolis meters split the air flow between two parallel u-shaped tubes. When there is no flow, the tubes are made to vibrate at their resonant frequency. Flow through the tubes alters this frequency at the inlet and outlet to the meter in proportion to the mass flow rate through them. Condensate or any other mass in even one of the tubes will show a non-existing mass flow rate.

Figure 21: Lab Test Runs (August 2020) Condensation and Flow Cutoff Impacts

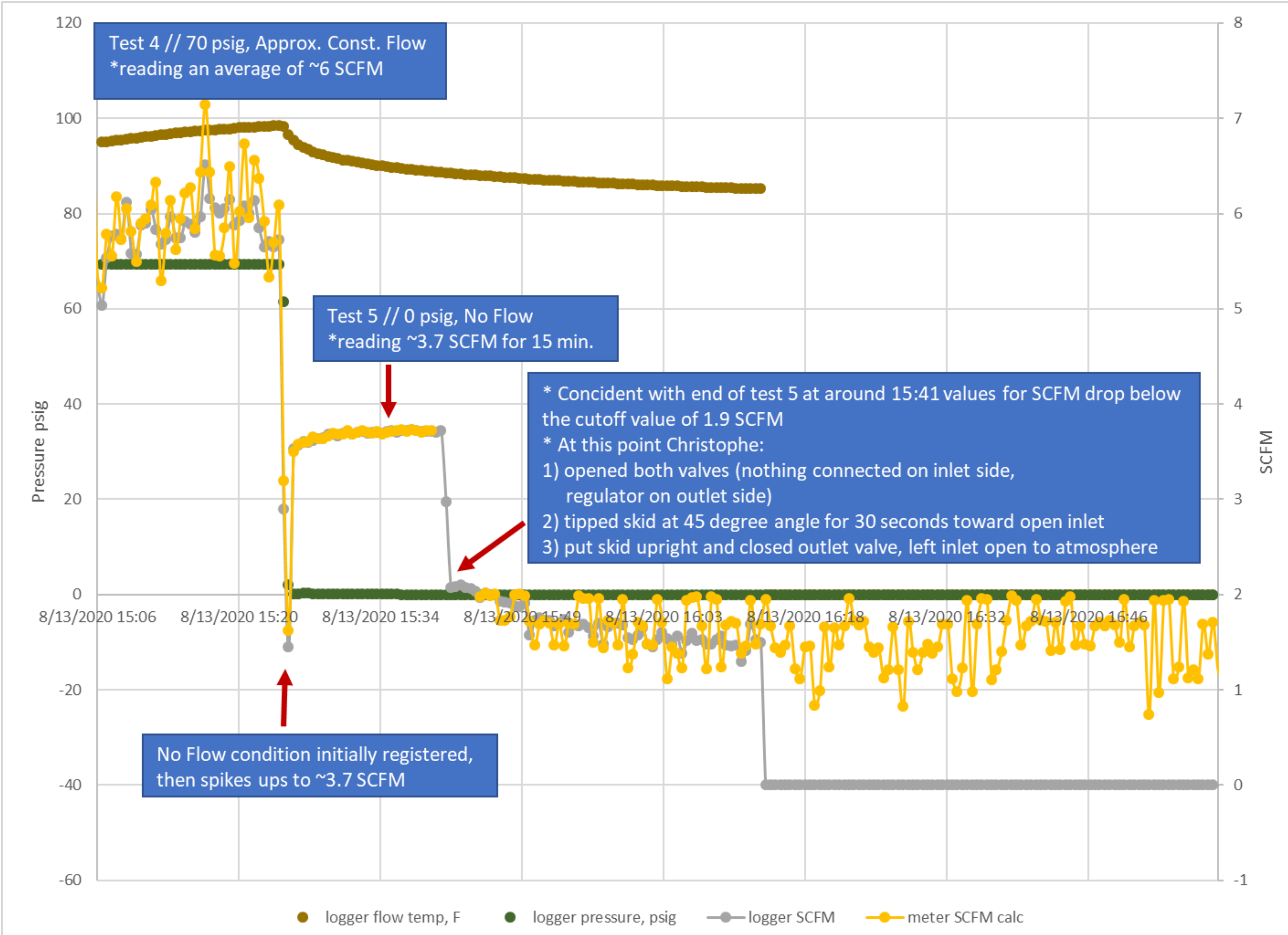

Pressure [psig] and SCFM plots during lab testing reflecting condensation and flow cutoff impacts

Source: GTI

Figure 22 shows the results of one of the “tilt” tests, wherein the skid was tilted to remove any collected condensate. By moving the skid, approximately 5 mL of condensate was removed and the SCFM and mass flow outputs (orange and blue plots) returned to showing no flow.

Figure 22: Tilt Tests — Flow Metering Condensation Tests (August 2020)

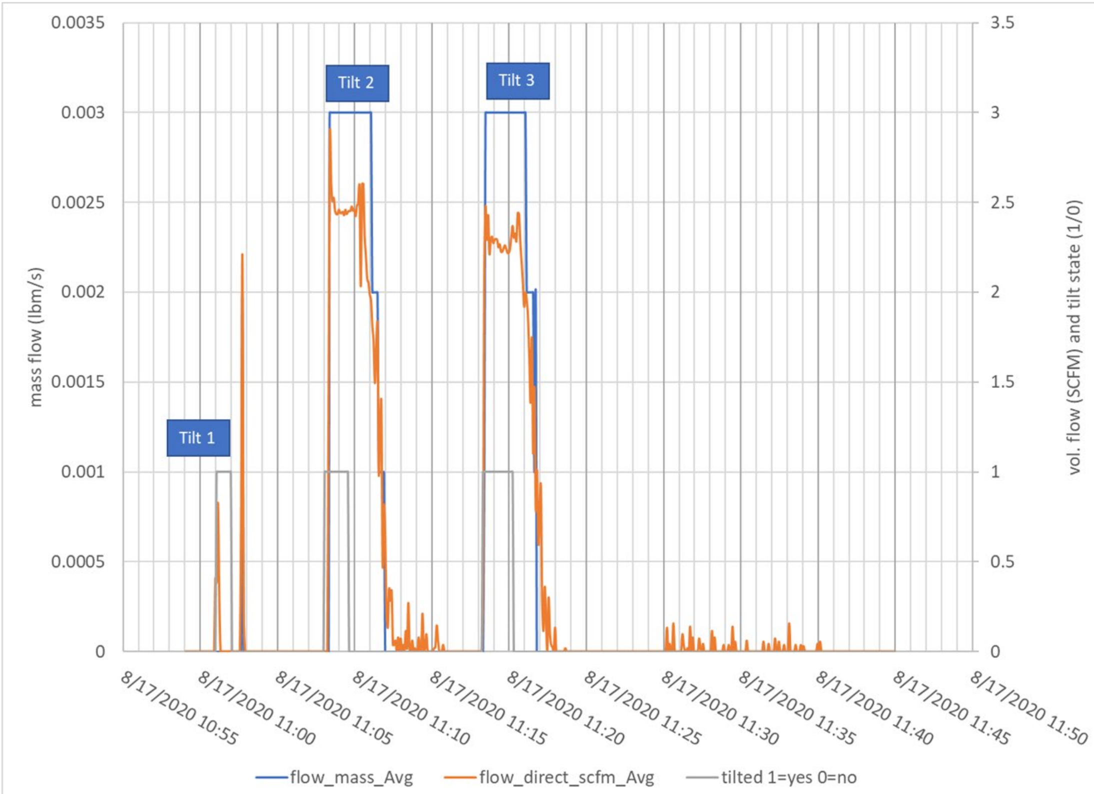

Mass flow rate time series plots of flow condensation lab tests

Source: GTI

Meter Verification and Alternatives

To further investigate the lower-than-expected flow, the project team used other methods of flow measurement. To do this, the project team decided to use a shop compressor (DeWalt Model D55168 Type 7) with a known rated flow rate, which was available at the Carnot testing site. Carnot had available and incorporated an Omega thermal dispersion mass flow meter (Omega Model FMA1844-A) and a variable area float style flow meter (Headland Model H271A-020) into the testing skid to compare against the coriolis and identify alternative metering options. A Quincy QPNC-25 refrigerated air dryer with a zero-loss drain[8] system was purchased and incorporated into the system to address the condensation issues.

The shop compressor was rated for 5.4 SCFM at 90 pounds per square inch, atmospheric (psia) under standard conditions (for example, at sea level and 68°F [20°C]). By derating the shop compressor’s performance for the altitude (assumed at approximately 87 percent of rated capacity) and adjusting to ACFM at the ambient conditions during testing, the shop

[8] Zero-loss refers only to maintaining the pressure in the line during the condensate purge cycle. It is likely that some compressed air would be lost during the purging cycle.

compressor was estimated to provide approximately 5.5 ACFM, inlet at 90 psia at the elevation of Carnot's shop in Reno, Nevada (approximately 4,500 feet above sea level, assumed barometric pressure of 12.49 psia).

Figure 23 shows data recorded on November 23 for the shop compressor at approximately 88 psia operating pressure. Assuming nameplate values, the shop compressor would theoretically provide around 5.5 ACFM, inlet at 90 psia (and therefore slightly more at 88 psia), but the coriolis flow meter was measuring approximately 3 ACFM, inlet and the Omega was measuring approximately 12 ACFM, inlet. The spot check suggested that the coriolis meter was closer to the assumed flow rate of the shop compressor, but it was still below the expected flow rate.

Additionally, the recorded mass flow values (not pictured in Figure 22) were close to the instrument's mass flow cutoff, registering 0.003–0.004 lbm/s with the cutoff value of 0.00238 lbm/s. Conversely, the Omega flow meter was reading approximately two times higher than the expected flow rate and was assumed to require additional calibration. It is possible that the thermal dispersion meter may have been damaged by condensation observed in the unit during earlier test runs without the dryer in place.

The mechanical variable area float style flow meter was closest to the expected flow rate, but the float style meter had no analog output to use with the monitoring system (only visual reading) and was used solely as another point of comparison.

Figure 23: Shop Compressor — Meter Comparisons

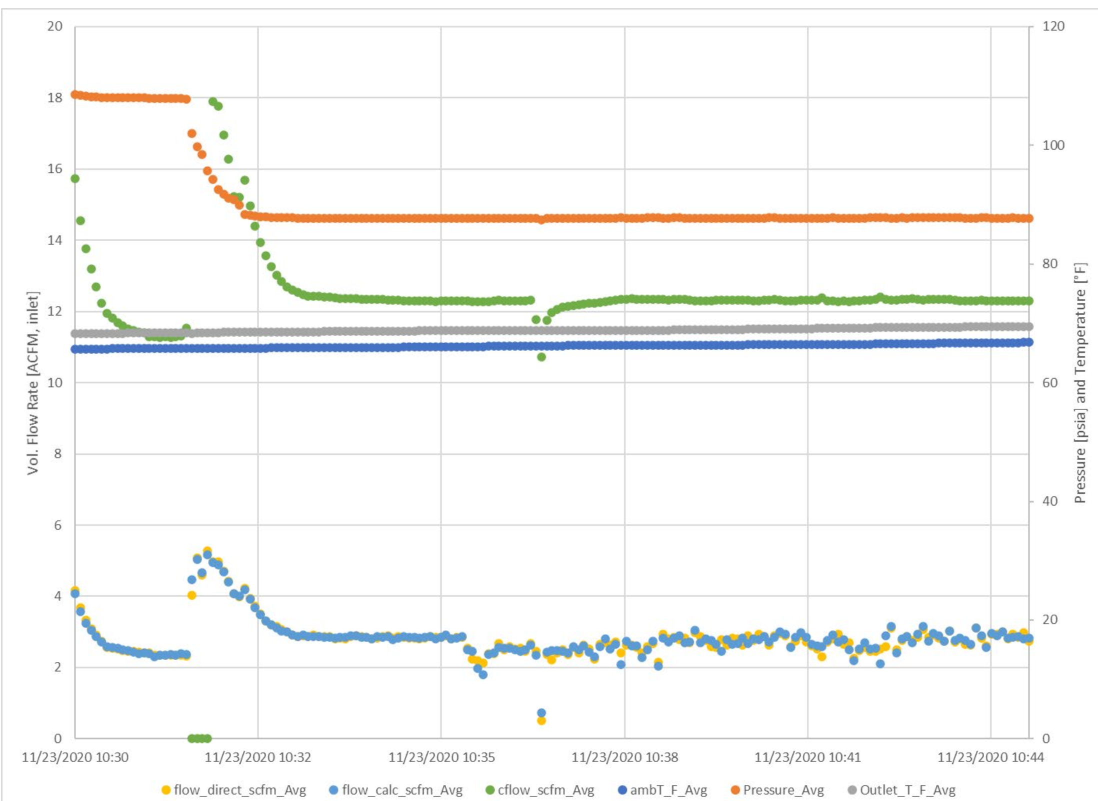

Inlet volumetric flow rate (ACFM) and pressure (psig) and temperature (F) plots for different meter comparisons.

Source: GTI

These test results suggested that the given thermal dispersion flow meter was not a suitable replacement for the coriolis flow meter and likely needed to be calibrated again. Additionally, the tests suggested the coriolis flow meter was oversized for the Carnot prototype and that condensation was a potential metering issue. The remainder of the lab testing period was used to provide data for operational improvements to ensure that the compressor would operate reliably in the field for long durations. In parallel, GTI specified a new mass flow meter for the monitoring system with a lower measurement range that would be slightly above the cutoff for the coriolis meter.

Facility, Design, and Equipment Barriers

During the July 13, 2020, run, the motor overloaded and was operating above the rated horsepower (nameplate 15 HP motor operating at around 20 HP), which subsequently caused some electrical issues. On July 22, 2020, it was determined that the cause for the overloading was a failure in the water balance tank. Additional modifications were made to the pitot tube, fill, and static vane return throughout the month of August and several leaks were addressed as the compressor was not able to match the data from the July 13, 2020, run. On August 27, 2020, it was decided that the motor was damaged, as it continued to operate with a power input above its rating while producing little air.

A new 20 HP motor was ordered to replace the existing 15 HP motor and tests were run in mid-September to get the new motor integrated into the system. During the September runs, Carnot determined that a decrease in viscosity due to heat management was causing issues with the balance of water in the compression drum, thereby adversely affecting the performance of the machine. Given the dynamic behavior of the system as the working fluid/cooling water heated up, the decision was made to integrate a PLC to dynamically control the balance of water in the drum to keep it within the ideal parameters.

The PLC module was installed at the end of September 2020, but additional compressor mechanical issues and panel breaker limits affected operation through the end of October 2020. Electrical issues subsided at the end of October 2020, and an external heat exchanger (condenser unit) was added to help manage the heat produced by the compressor. In November 2020, it was decided that Carnot would focus on design changes to help drive up airflow and efficiency and use the time to aid development of the prototype through to commissioning at the host site in March 2021. During this period of development, the proposed design evolution necessitated other changes to the compressor drum and the decision was made to revert to the original components used in the July 2020 testing in advance of field deployment.

Remote Operation

The project team had also planned on providing remote start-up/shutdown of the unit, but this effort was abandoned due to the ongoing troubleshooting, design, and control changes mentioned previously as well as a limited cell signal at the field test site. Ultimately the unit was able to operate in an unsupervised manner, with the PLC limiting the operation of the compressor to the hours of operation of the host site. On a related note, alarms based on measurement points, such as water temperature, were incorporated to provided notice to the project team of any off-operating conditions or drastic changes in ambient conditions.

Field Testing Results

Commissioning and Lessons Learned

The prototype was installed in the shed housing the backup compressor for Litton Engineering Laboratories in Grass Valley, California, as detailed in the Testing Sites section of Chapter 2. The prototype was installed in late March 2021 and removed in November 2021. It was plumbed into Litton's existing compressed air system, which supplies compressed air to its machine shops, just upstream of its collection tank and in parallel with both its primary rotary screw compressor and its backup piston compressor. It was programmed to operate from 7:00 a.m. to 5:00 p.m. on weekdays and was expected to operate in tandem with the primary compressor. Litton's compressed air system operates with a cutoff pressure of 113 psig and the FD3 was programmed accordingly. The following sections describe the hurdles overcome and the lessons learned during commissioning and operation during field testing.

Water Management

The initial FD3 design had a single manifold at the tail end of the compressor skid through which excess water from various locations on the unit passed. This made shut-down drainage too slow, so a sump was incorporated under the compressor into which the drum drained directly. A small sump pump was added to push the discharge water through the manifold and out to the drain. This addition may be incorporated into future iterations.

Heat Management

Water from the compression drum was extracted and routed through a cooling loop, out of the compressor skid to a remotely located heat exchanger (radiator and fan) to reject most of the heat produced during operation. However, during testing the prototype was installed in a small, poorly ventilated cement block shed and the combination of warm ambient temperatures and the portion of heat generated by the compressor that was not evacuated by the cooling loop caused the temperature inside the shed to reach 110°F during operation, creating thermal troubles for the electrical components. As a solution, a fan was bolted over the small louvered window of the shed to help manage the inside temperature. As the ambient temperature dropped, the overheating became a non-issue.

Drum Overfill

This was the biggest operational issue with the FD3. Start-up involved spinning up the drum and adding water until the annular lake was deep enough to reach the pitots and the SVR inlets. Once the water depth reached the SVR inlets, the required current ramped up steeply and became very sensitive to changes in the water level. The PLC used the motor current to control the water level. An overfill situation could occur if too much water was added, increasing the current to an unacceptable level. A soak/ramp was programmed into the PLC to mitigate this, with some success, but variability during start-up was just enough to cause the overfill fault to occur too frequently for industrial purposes. The SVR concept was abandoned on subsequent embodiments, eliminating this issue.

Inshot Current

The initial energy required to spin the drum up to the desired speed caused a spike in current. The standard motor starter (coil) in the FD3 brought the motor to speed within a few seconds. The coil and breaker were insufficient to handle the current spike if the drum had water in it at start-up and could trip the breaker. This required that the drum be fully drained between runs. The addition of a soft starter or a variable frequency drive eliminated this issue on subsequent embodiments.

Start-up Interval

At field deployment, the FD3 spindown and drain time required approximately 5 minutes before restarting could occur. Also, the ramp/soak function controlling the introduction of water into the drum at start-up took approximately 4 minutes to bring the compressor to steady state, resulting in a nearly 10-minute cycle time. Addition of the sump shortened this delay by reducing the drum drain time. The addition of a soft starter or variable frequency drive in subsequent embodiments significantly reduced the interval by fully eliminating the 5-minute drain period. As stated in the Drum Overfill section above, more recent embodiments also eliminated the overfill issue, which eliminated much of the ramp/soak time necessary to reach steady state.

Pitot Rebuilds

The pitot body was a 3D printed nylon part that was significantly modified during testing. The modifications included incorporating the bronze pitot heads and copper tubing into the printed part. The repairs for these modifications were done using a two-part epoxy, which holds up relatively well for prototype purposes but erodes over 50–70 hours of operation. This would not have been an issue had the pitot body been made entirely of the 3D printed nylon and not repaired with epoxy. The pitots were rebuilt twice while the compressor was in the field. The pitot design on subsequent embodiments eliminated the use of metal inserts, resolving this issue.

Hydraulic Resonance

During its start ramp, the FD3 frequently experienced a harmonic resonance[9] through one band of frequencies as it spun up, resulting in significant vibration for 10 seconds or so before smoothing out. Once in steady state operation, the FD3 tended to surge and subside due to the turbulent internal hydraulics and slight variations in water level. The PLC worked to keep the operation at a current set point, but the internal hydraulics of this iteration were very sensitive to variation. A redesign of the internals in subsequent embodiments largely resolved this issue.

[9] Harmonic resonance refers to a wave frequency across nodes in which an external force or system forces another system to vibrate with greater amplitude. This can pertain to equipment vibration along with sound emittance.

Field Testing Performance Results and Analysis

Data Summary

A summary of the performance results from field collected data is provided in Table 12. The data used was collected over 571 compression fill events, excluding the start-up events to come to system pressure. The data shows the average capacity to be 0.63 ACFM, inlet (standard deviation [SD]=0.09) when operating with an approximately 98 psig cut-in and 113 psig cut-out pressures at the Litton Engineering facility. The average isentropic efficiency was calculated to be approximately 0.31 percent (SD=0.04 percent) and the average specific power was calculated to be 3,091 (SD=529) kW/100ACFM under those same operating conditions.

The power consumption included measurements from the motor and ancillary systems (for example, controls, pumps, PLC, and other parts) as well as an assumed power of 150 W based on measured values for the heat rejection loop fan. The dryer power consumption was not included.

The averaged mass flow from which the ACFM at inlet conditions was calculated via the state variable approach is described in the Calculation Methods subsection under the Mass Flow Rate — State Variable Approach section in Chapter 2. The following section compares the mass flow measurements obtained with the flow meter and calculated using the state variable approach.

Lastly, the polytropic index was calculated to be 1.02 (SD=0.00572), suggesting that the process was very nearly isothermal as opposed to isentropic (for example, an index of 1.4).

Table 12: Field Test Data Summary

Description	Value	SD	Unit
Number of Fill Events	571	-	dimensionless
Average Fill Mass Flow	0.293	0.043	g/s
ACFM @ Inlet Conditions	0.63	0.09	ACFM, inlet
Standard Atmospheric Pressure (@ Sea Level)	14.6959	-	psia
Assumed Atmospheric Pressure (@ Elevation)	12.3	-	psia
Ambient Temperature	83.1	10.6	°F
Delivery Pressure	112.8	1.0	psig
Specific Power	3091	529	kW/100ACFM
Isentropic Efficiency	0.31	0.04	%
Isothermal Efficiency	0.30	0.04	%
Polytropic Index	1.02	0.00572	dimensionless

Source: GTI

There was also some measured impact on the compressor's capacity for data collected with warmer ambient temperatures, due to the ability of the system to reject the heat of compression and the implications thereof on the system's operation, as mentioned in the design reports (Figure 24).

Figure 24: Ambient Temperature Impact on Capacity

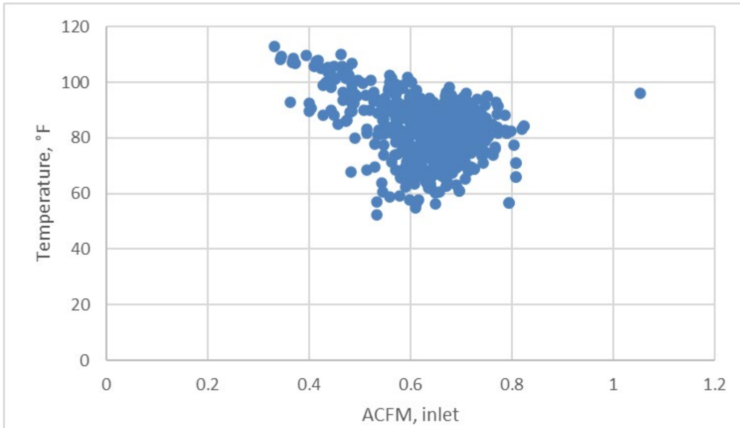

Source: GTI

State Variable Approach Validity Analysis

Data from 28 compression events was obtained to provide a comparison of the mass flow measurements obtained with the flow meter against those derived using the state variables of the compressed air in the air receiving tank. The data points for metered and calculated values for mass flow are plotted below in Figure 25.

Despite a small number of data points, the data points may be considered to have an acceptable correlation, as field data rarely had very high R^2. There were some outliers that affected the R^2 value, but the slope of the fit was close to what one would expect (for example, y=1 x) despite the spread of data points. There was also a slight offset reflected by the intercept (b=0.0354 g/s), showing that the mass flow meter readings may have been slightly higher than what was calculated using the state variable approach.

Figure 25: Metered Mass Flow Comparison — Line of Equality

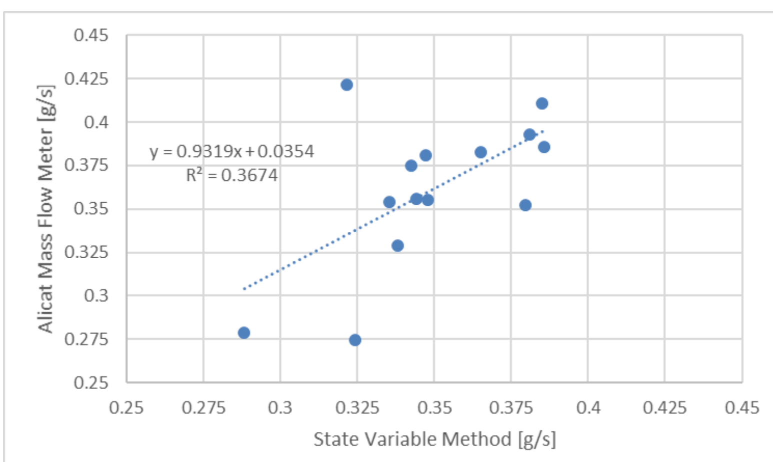

Mass flow rate (g/s) vs state variable method (g/s) plot for metered mass flow comparison.

Source: GTI

A limits of agreement analysis (or Bland-Altman/Tukey plot) provides a useful measure for comparing the differences between individual results measured by two different methods or two different instruments, such as in this study; it is useful when, for example, calculating from state variables (pressure, temperature, and volume) versus measuring mass flow directly with the laminer flow element (LFE) mass flow meter. This analysis method accounts for both systematic and random error and has gained popularity in the analytical chemistry and medical fields when new measurement techniques are being examined (for instance, when a new type of blood oxygen sensor is introduced to the market).

The analysis started with plotting the difference between the same measurement made with two different methods (for example, measurement pairs) against the mean of the measurement pair (blue data points in Figure 26). This would, by itself, show any bias between the two methods across the measurement range.

Next, the mean of all differences *M* — represented by the purple dashed line in Figure 26 — as well as the interval of 1.96 standard deviations (95 percent limits of agreement) of the measurement differences *M±2SD* — red dashed lines in Figure 26 — was plotted. These bounds represent the limits in which the new method or instrument agreed with the other.

From this plot, the project team could infer that most of the differences for this set of data between the two measurement approaches were within the established limits (with one exception), suggesting that the two methods (state variables approach and LFE flow meter) were very likely interchangeable.

Figure 26: Limits of Agreement Between State Variable Derived and Metered Mass Flow Rate Measurements

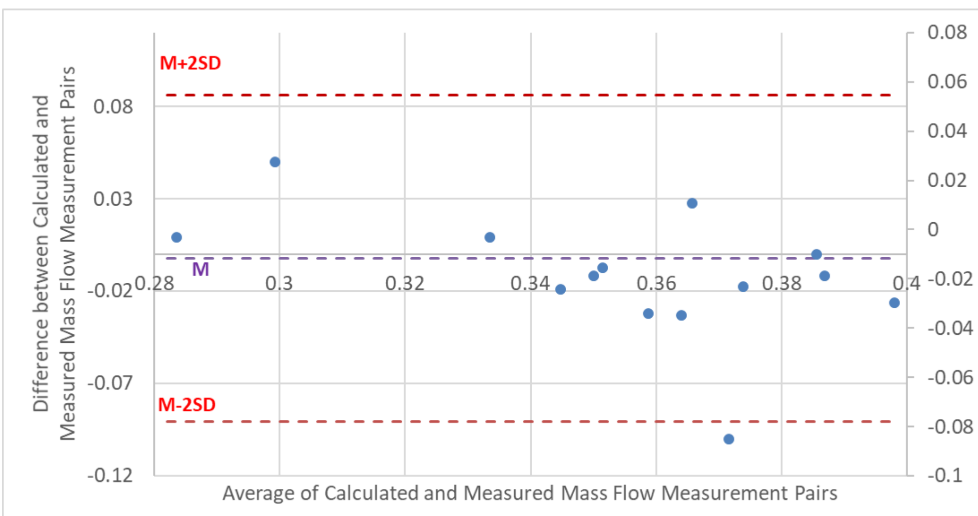

Plotted differences for calculated and measured mass flow measurement pairs.

Source: GTI

An additional observation may be made that the squared variance of the residuals between the two measurement methods (shown in Table 13 as RMSE) is an order of magnitude smaller than the measurements themselves and was on the order of the standard deviations of both sets of data as well.

Table 13: Mass Flow Data Comparison Summary

Description	Value	Unit
N* Metered Flow Events	28	dimensionless
Meter Mass Flow Avg	0.361	g/s
Meter Mass Flow SD	0.042	g/s
Mass Flow Accuracy	0.003	g/s
State Mass Flow Avg	0.349	g/s
State Mass Flow SD	0.028	g/s
RMSE State vs Meter	0.035	g/s

*N Number
Source: GTI

Figure 27 shows a plot for one of the 28 data points used for the comparison of the LFE mass flow meter to the state variables approach to mass flow measurement covered in the Mass Flow Rate – State Variable Approach subsection of the Calculation Methods section of Chapter 2. A plot like the one below was produced for all tank fill/drain events to assist with data munging.

The first subplot shows the air receiving tank's gauge pressure in psig and the cumulative motor electricity in Wh, and the second subplot shows the cooling loop temperature, compressed air dew point temperature, tank air temperature, and ambient air temperature. Please refer to Figure 12, Field Measurement Point Schematic, for the sensor locations during the field-testing phase.

Figure 27: Field Testing Data Slice

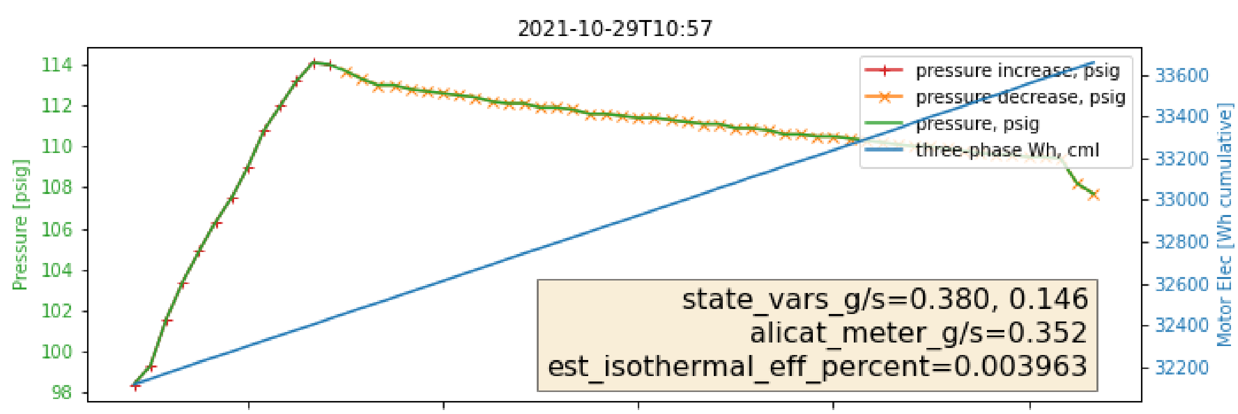

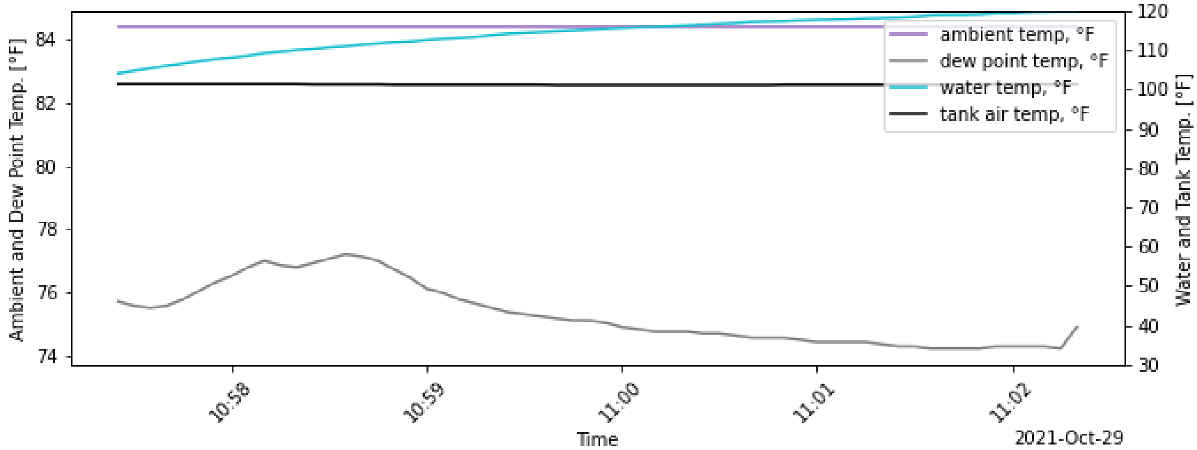

(Top subplot) Pressure (psig) and motor electric consumption (Wh) and (bottom subplot) ambient and dew point temperature (F) with water and tank temperature (F) time series field test results

"State_vars_g/s" is the mass flow rate in grams per second, calculated using the state variables tank pressure and temperature, as well as the known volume of the air receiving tank.

"Alicat meter_g/s" is the average mass flow rate measured by the Alicat flow meter.[10]

"Est_isothermal_eff_percent" is the isothermal efficiency written as a fraction (for example, 0.3963%).

Source: GTI

[10] There are two values for the averaged mass flow rate. The first, "state_vars_g/s", is for the "fill" portion of the air receiving tank (red "plus" sign markers), where there is only flow into the tank. The second is for the drain of the tank (denoted by yellow x sign markers), where there is both flow into and out of the tank. The calculated mass flows are different because they are based solely on the initial and final values of the tank's air pressure and temperature. The second value 0.146 should be ignored.

The data for the 28 tank fill events used in the mass flow measurement comparison is shown in Table 14.

Table 14: Results With LFE Meter Measured Mass Flow

Start Time	Mass Flow (State Vars)	Mass Flow Alicat	Amb. Temp.	T1_F	T2_F	P1	P2	Vol. Flow at Inlet	Specific Power	Poly. Index	Isothermal Eff.	Isentropic Eff.
YYYY-MM-DD HH:MM:SS	g/s	g/s	°F	°F	°F	psig	psig	ACFM	kW/ 100ACFM	N/A	%	%
2021-10-26 12:02:50	0.386	0.386	56.6	70.9	71.7	98.9	114.1	0.79	2468.238	1.04	0.37%	0.38%
2021-10-26 13:50:15	0.324	0.274	73.2	91.5	91.5	98.6	113.9	0.69	2769.393	1.02	0.33%	0.34%
2021-10-27 08:34:05	0.335	0.354	60.8	70.8	71.9	99.0	113.4	0.70	2779.438	1.04	0.33%	0.33%
2021-10-27 08:43:50	0.321	0.422	62.9	78.2	79.1	98.7	113.7	0.67	2882.403	1.04	0.32%	0.32%
2021-10-27 08:55:05	0.385	0.411	66.0	84.4	85.0	98.7	114.2	0.81	2381.994	1.04	0.39%	0.39%
2021-10-27 09:04:50	0.344	0.356	68.8	88.3	88.8	98.3	113.4	0.73	2651.859	1.04	0.35%	0.35%
2021-10-27 10:12:40	0.347	0.381	78.8	98.7	99.1	98.4	113.9	0.75	2551.048	1.03	0.36%	0.37%
2021-10-27 10:53:15	0.365	0.382	81.9	101.6	101.9	98.8	113.9	0.79	2433.589	1.03	0.38%	0.38%
2021-10-26 12:02:50	0.386	0.386	56.6	70.9	71.7	98.9	114.1	0.79	2468.238	1.04	0.37%	0.38%
2021-10-26 13:50:15	0.324	0.274	73.2	91.5	91.5	98.6	113.9	0.69	2769.393	1.02	0.33%	0.34%
2021-10-27 08:34:05	0.335	0.354	60.8	70.8	71.9	99.0	113.4	0.70	2779.438	1.04	0.33%	0.33%
2021-10-27 08:43:50	0.321	0.422	62.9	78.2	79.1	98.7	113.7	0.67	2882.403	1.04	0.32%	0.32%
2021-10-27 08:55:05	0.385	0.411	66.0	84.4	85.0	98.7	114.2	0.81	2381.994	1.04	0.39%	0.39%

Start Time	Mass Flow (State Vars)	Mass Flow Alicat	Amb. Temp.	T1_F	T2_F	P1	P2	Vol. Flow at Inlet	Specific Power	Poly. Index	Isotherm al Eff.	Isentropi c Eff.
2021-10-27 09:04:50	0.344	0.356	68.8	88.3	88.8	98.3	113.4	0.73	2651.859	1.04	0.35%	0.35%
2021-10-27 10:12:40	0.347	0.381	78.8	98.7	99.1	98.4	113.9	0.75	2551.048	1.03	0.36%	0.37%
2021-10-27 10:53:15	0.365	0.382	81.9	101.6	101.9	98.8	113.9	0.79	2433.589	1.03	0.38%	0.38%
2021-10-29 08:57:10	0.288	0.279	67.5	76.5	77.0	99.0	111.4	0.61	3214.751	1.03	0.28%	0.29%
2021-10-29 09:35:25	0.381	0.393	70.9	85.5	86.2	98.1	113.5	0.81	2374.542	1.04	0.39%	0.39%
2021-10-29 09:47:35	0.348	0.355	73.7	91.6	92.3	98.5	113.9	0.74	2627.114	1.04	0.35%	0.35%
2021-10-29 10:05:55	0.343	0.375	78.3	98.1	98.6	98.5	113.8	0.74	2607.009	1.03	0.35%	0.36%
2021-10-29 10:25:40	0.338	0.329	82.2	102.7	103.1	98.7	113.9	0.73	2628.480	1.03	0.35%	0.35%
2021-10-29 10:57:25	0.380	0.352	84.4	101.4	101.3	98.4	114.0	0.82	2326.301	1.02	0.40%	0.40%
2021-10-29 08:57:10	0.288	0.279	67.5	76.5	77.0	99.0	111.4	0.61	3214.751	1.03	0.28%	0.29%
2021-10-29 09:35:25	0.381	0.393	70.9	85.5	86.2	98.1	113.5	0.81	2374.542	1.04	0.39%	0.39%
2021-10-29 09:47:35	0.348	0.355	73.7	91.6	92.3	98.5	113.9	0.74	2627.114	1.04	0.35%	0.35%
2021-10-29 10:05:55	0.343	0.375	78.3	98.1	98.6	98.5	113.8	0.74	2607.009	1.03	0.35%	0.36%
2021-10-29 10:25:40	0.338	0.329	82.2	102.7	103.1	98.7	113.9	0.73	2628.480	1.03	0.35%	0.35%
2021-10-29 10:57:25	0.380	0.352	84.4	101.4	101.3	98.4	114.0	0.82	2326.301	1.02	0.40%	0.40%

Source: GTI

CHAPTER 4: Technology Transfer Activities

A final technology and knowledge transfer plan was prepared for the California Energy Commission to outline the planned activities for supporting the sharing of knowledge gained and lessons learned throughout this project. The core of these activities entailed distributing information to the following target audiences:

- Public
- Government Organizations
- Commercial Industries
- Engineers
- Professional/Trade Organizations
- Utilities

The objective of this outreach is to educate the target audiences on the novel technology and its potential for a deep impact through energy savings and increased reliability across industries requiring air compression.

Website

The Carnot Compression team has created a website (carnotcompression.com) that describes the technology of the FD3 prototype compressor demonstrated in this project. The website describes the oil-free and near-isothermal compressor technology by means of a high-quality animated video. Additionally, the website outlines the mission of the Carnot team and the technology's potential global impact by tackling the exorbitant energy consumption of conventional industrial air compressors.

The website features news about the technology's development and gives visitors the opportunity to subscribe to an email newsletter; to date there are 2,429 subscribers. Methods of contacting the project team and ways to invest are also highlighted. In 2021 the website had 6,700 visits and 11,000 page views, with 5,600 unique visitors.

The Carnot team also uses StartEngine for online public fundraising and to broadcast the technology for investors. As of February 22, 2022, the StartEngine campaign had raised $685,774 with 870 investors. The URL for the StartEngine webpage is: https://www.startengine.com/offering/carnot-compression

Fact Sheet

A two-page fact sheet was composed to rapidly convey the project's technology to a general audience. This document features a high-level description along with benefits of the project. For transparency, project details such as state financial support and contact details for GTI and the California Energy Commission are included.

Webinar

A one-hour presentation was given to the California Energy Commission contract agreement manager on March 25, 2022. The webinar featured the Carnot FD3 compressor technology, applications, and testing results. Only the project team and the commission agreement manager attended.

Media Podcasts and Online Broadcasts

NGV World Podcast With Ricardo Carmona

Carnot Compression CEO and Co-Founder Todd Thompson was featured on the NGV World Podcast with Ricardo Carmona, released on June 15, 2020. The NGV World Podcast broadcasts state-of-the-art technology within the gas industry to a large audience. In this podcast, Thompson describes the technology details of the FD3 compressor, illustrates how the technology was developed, and discusses the direction in which the technology is headed.

Fundraising Radio Podcast

The Fundraising Radio Podcast featured Carnot Compression CEO and Co-Founder Todd Thompson in an episode released on July 16, 2021. The theme revolved around the funding of Carnot Compression and its three main capital sources, including equity crowdfunding, grants, and friends and family. Thompson was selected for this episode because of his unique insight on the financial aspect of developing the novel, near-isothermal compression technology.

Small Business Network

Carnot Compression was mentioned in an episode of the Small Business Network, published on July 8, 2020. This episode highlighted the technology's energy savings potential and provided resources for investing in Carnot.

Media Publications

New Atlas

The website New Atlas featured Carnot in an article on July 18, 2020, which illustrated the innovative Carnot technology relative to outdated conventional air compressor designs.

Interesting Engineering

Carnot Compression was featured in an article released on July 20, 2020, by Interest Engineering.

Benzinga

Carnot Compression was featured in two articles in Benzinga, which were published on December 14 and 20, 2021. The first article highlights the problems solved by Carnot in air compression and in the environment. The second article analyzes the potential impact the

Carnot technology can have across the global compressed air market and how it can displace conventional air compressor technology.

Conference Events

Compressed Air Best Practices Forum

The Carnot team attended the Compressed Air Best Practices Forum in Nashville, Tennessee, on October 14 and 15, 2019. Here, the Carnot team met with multiple potential original equipment manufacturers and component supplier partners. This conference, co-sponsored by the Compressed Air & Gas Institute (CAGI), was devoted to optimizing the technologies powering modern plant automation and featured programs from industry leaders.

Plug and Play Tech Center

Carnot Compression delivered a presentation on the Carnot technology at the Plug and Play Tech Center in Sunnyvale, California, on October 11, 2019. The Plug and Play Tech Center is the world's largest early-stage investor, accelerator, and corporate innovation platform.

Start-up Investment and Community Capital Expo

The Carnot team was a featured presenter at the Start-up Investment and Community Capital Expo at California State University, Monterey Bay, on September 28, 2020. This conference is the region’s largest showcase of emerging technologies companies. By facilitating the connection between investors and companies, this conference intends to expedite technology growth.

Frost & Sullivan Oil & Gas Innovation Council

Carnot Compression presented at the Frost & Sullivan Oil & Gas Council on November 4, 2020, illustrating its novel compressor technology. This conference spotlights innovations, new business models, processes, and best practices from all industries that have the potential to change the oil and gas industry and put the members on the path for transformational growth.

Professional Societies

ASME

The American Society of Mechanical Engineers (ASME) published an article on Carnot Compression on September 3, 2020. This article highlighted the Carnot engineering team and the novel, near-isothermal design. Carnot’s mission was also featured, along with a history of the company.

Government Organizations

Oakridge National Laboratory

In a new partnership, Carnot Compression is working with Oakridge National Laboratory. This collaboration is aimed at developing and improving the Carnot technology through computational fluid dynamics[11] studies.

Utilities

The Carnot team has worked with utilities, including Pacific Gas and Electric Company, San Diego Gas & Electric Company, and Southern California Edison, on customer outreach efforts. These relationships have helped shape the market and customer outreach of Carnot to drive the technology toward areas of potential impact.

Corporate and Industry Partnerships

The Carnot team has met with manufacturers, such as PEKO, to produce this technology. Additional confidential discussions have been held with multi-national manufacturers and industry leaders.

On February 11, 2021, Carnot announced its first partnership in the dairy industry with Tilla-Bay Farms of Tillamook, Oregon, for its robotic milking operations. Tilla-Bay Farms is home to the first 24/7 robotic milking system in the western United States.

Beta Customer — Tilla-Bay Farms/Dairy Specialists Incorporated

Carnot has received multiple inquiries regarding applying the technology for robotic milking, specifically for Lely machines. Customers currently use oil-free scroll compressors and are experiencing expensive maintenance and a relatively short operating life, leading to frequent purchases of new compressors to run the robots. With one moving part for the compression process, Carnot's design is well-suited to withstand the 100 percent duty cycles demanded by the industry. Carnot believes it can offer a long-lived, 100 percent duty cycle oil-free compressor that will lead to increased uptime and lower lifetime operating costs for dairy customers.

Carnot will install a beta test unit at Tilla-Bay Farms in Tillamook Oregon in the first half of 2022. Dairy Specialists Incorporated will provide support for the installation and the ongoing operations and maintenance of the machine. This beta test will allow Carnot to demonstrate proof of functionality in this targeted customer application while it continues to refine the product and increase energy efficiency. Dairy Specialists has a broad footprint in the western United States and could be an early commercialization partner for the dairy industry. On a broader scale, there could be an opportunity to form a relationship with Lely to custom design and package the compressor for Lely robotic milking machines.

[11] Computational fluid dynamics is a computer-based numerical analysis used to model and analyze fluid flow problems.

CHAPTER 5: Conclusions and Recommendations

During the project, an alpha prototype compressor was designed and built for testing in both laboratory and field-site environments. The product was successfully installed in a real-world setting and reliably produced compressed air in a very nearly isothermal manner at commercially relevant pressures. While the results of this project demonstrated that the alpha version of the compressor did not meet or exceed the efficiency of currently available commercial products, opportunities for improving system performance were identified and are being incorporated into the beta version compressor for further study under contract EPC-21-017, a $2,028,350 grant under the California Energy Commission BRIDGE program, beginning in the second quarter of 2022.

Lessons Learned and Applied

The engineering design tasks of the current research provided many learning opportunities for Carnot, which were incorporated into the final prototype design to improve compression efficiency and minimize the complexity of the system. These developments are covered in the Engineering Design section of Chapter 2, Project Approach. Beyond the engineering design tasks, there were several lessons learned through both lab and field testing that also contributed to additional insight regarding materials selection, motor inrush current, heat/water management and control system approach (that is, physical logic with switches and other analog sensors vs. a programmable logic controller). A detailed review of each topic is provided in the Commissioning and Lessons Learned section of Chapter 3, Project Results.

Suggestions for future study of the system may include measuring the heat being rejected from the system, as it may be potentially useful low-grade heat that could be used for some process heating applications such as preheating water or a product stream. It would also be beneficial to development to conduct additional measurements of the wastewater from the process to help inform the materials selection, purge water conveyance/treatment, maintenance guides, and installation requirements for the system.

Next Steps

Carnot Compression Inc. is expected to begin the contract EPC-21-017 project. This research and development project will further advance the Carnot compressor technology to commercial readiness by optimizing the compressor's air-end design to unlock its full energy savings potential and by applying the improved design to a series of field tests for a beta version of the compressor.

EPC-21-017 builds upon the research and development completed under this agreement as well as work funded by National Science Foundation Small Business Innovation Research Phase I and II awards. The primary goals for EPC-21-017 are to optimize the air-end design of the Carnot Compressor® and demonstrate the improved design in preparation for commercial product launch. Key objectives are to 1) incorporate design improvements into beta units ranging from 5 HP to 25 HP; and 2) conduct field tests at various customer sites, representing a diversity of operating environments in Northern and Southern California. Proving both the efficiency enhancements from the next design iteration, along with testing in multiple relevant environments with different customer requirements, will accelerate the path to commercializing the Carnot Compressor.®

CHAPTER 6: Benefits to Ratepayers

By removing the heat throughout the compression step, the energy required to compress air from near atmospheric pressure to approximately 100–150 pounds per square gauge can be reduced by 20 percent or more compared to commercial air compressors such as piston, screw, or scroll designs. This improvement is expected to significantly increase the efficiency of industrial air compression through energy savings and increased reliability across industries requiring air compression. Carnot's novel near-isothermal design has the potential to displace conventional air compressor technology and can make a significant difference in the compressed air market, not only in California and nationwide but also globally. Improvements in compressing air will, in turn, significantly reduce energy requirements for air compression — again, statewide, nationally, and globally. Carnot believes the technology can be applied to other compressor applications in the future, such as compression of natural gas in transmission and distribution systems, leading to additional energy savings across many industrial gas applications.

GLOSSARY AND LIST OF ACRONYMS

Term	Definition
air receiving tank	A storage tank that is either packaged with a compressor or installed separately as part of a compressed air system.
alpha prototype	The initial iteration of the prototyping process; serves as a "proof-of-concept" meant to test and demonstrate the fundamental designs upon which a finished product is based.
California Energy Commission BRIDGE	A program designed to: 1) help start-up companies minimize the time between the end of their successful publicly funded project and the availability of new public funding; and 2) mobilize more early-stage capital in the clean energy space by providing non-dilutive, matching investments in promising clean energy companies alongside investors and commercial partners.
energy dispersive x-ray (EDX)	A technique associated with electron microscopy based on generation of characteristic x-rays used to analyze elements of a specimen.
heat of compression	The increase of heat for a compression process. As work is done on a fluid, energy is transferred to the fluid which may be observed through an increase in temperature.
ideal gas law	A relationship among pressure, volume, temperature, and quantity of gas. An ideal gas approximates the behavior of real gases with the following assumptions: 1) ideal gas molecules do not attract or repel each other, and 2) ideal gas molecules themselves take up no volume. In molar form, the ideal gas law can be expressed as pressure (P) multiplied with volume (V) set equal to the product of temperature (T), number of moles (n), and the universal gas constant (R) or $P*V = n*R*T$. In this molar expression, the gas constant is expressed as $R = 8.31$ J/(K*mol), where J is energy in joules, K is temperature in kelvin, and mol is number of moles.
Independent System Operator (ISO)	A neutral operator responsible for maintaining instantaneous balance of the grid system. The ISO performs its function by controlling the dispatch of flexible plants to ensure that loads match resources available to the system.
isentropic efficiency	The ratio comparing an actual process and an ideal isentropic process, where the same system is assumed to be both adiabatic and reversible. For a compression process, the isentropic efficiency is the theoretical work input to an ideal system divided by the actual work of the compressor.
isothermal process	A process where temperature is constant.
joule (J)	A unit of energy or work equal to the amount of work done when the point of application of force of 1 newton is displaced 1 meter in the direction of the force. It takes 1,055 joules to equal a British thermal unit. It takes about 1 million joules to make a pot of coffee.

Term	Definition
kelvin (K)	A unit of temperature also called the absolute temperature scale. The lowest or coldest temperature possible is 0 K, or absolute zero. The Kelvin scale can be related to other temperature units like Celsius and Fahrenheit. Kelvin and Celsius have the same incremental scale, wherein 1 unit Kelvin is equal to 1 unit °C. To calculate a temperature, add 273 to the Celsius temperature, wherein T(K) = T(°C) + 273.15.
laminar flow element	A flowmeter used to measure the flow of fluids through closed conduits.
mole (mol)	A unit measuring the amount of a substance. One mole is equal to 6.022 x 1023 particles. The term "particles" may refer to small objects such as atoms or electrons as well as any other object, independent of size.
National Science Foundation Small Business Innovation Research (NSF-SBIR)	The National Science Foundation's congressionally mandated program that funds start-ups to develop new technologies, often based on fundamental science or engineering, in need of research and development to create new products, services, and other scalable solutions.
natural gas vehicle	A vehicle that is powered by compressed or liquefied natural gas.
programmable logic controller	An industrial ruggedized computer that can be used for machine automation.
recirculation and energy recovery turbine (RERT)	A compressor component used to slow the water exiting the drain column to generate both shaft torque and sufficient head. The RERT component was replaced by the static vane return after design testing and iteration.
resistive temperature device (RTD)	A sensor used to measure temperature through a relationship between temperature and electrical resistance, often applied within thermal fluid systems.
scanning electron microscopy (SEM)	A method using electron microscopes to beam high-energy electrons to generate a variety of signals at the surface of solid specimens. The signals that derive from electron-sample interactions reveal information about the sample, including external morphology (texture), chemical composition, and crystalline structure and orientation of materials making up the sample.
soft starter	A type of motor that reduces the voltage during the starting of a motor, offering a gradual voltage increase for motor start-up.
specific power	The capacity-adjusted power consumption of a compressor operating at a given compression ratio, calculated by dividing the power consumed by the process by a unit of volumetric flow rate of air drawn into the inlet of the compressor. Specific power is typically expressed in kilowatts per hundreds of cubic feet in kW/100ACFM at a specified delivery pressure.

Term	Definition
standard cubic feet per minute (scfm)	The molar flow rate of a gas corrected to standardized conditions of temperature and pressure, thus representing a fixed number of moles of gas regardless of composition and actual flow conditions.
static vane return (SVR)	A component of the Carnot FD3 compressor used to reduce the power required to spin the compressor drum by maneuvering water flow.
thermocouple	A sensor used to measure temperature, frequently consisting of two joined dissimilar metal wires with free ends connected to a voltage-reading instrument that measures the difference in potential created at the junction of the two metals.
viscosity	The degree to which a fluid resists flow under an applied force.
ACFM	actual cubic feet per minute
ASHRAE	American Society of Heating, Refrigeration and Air-conditioning Engineers
ASMD	American Society of Mechanical Engineers
C	Celsius
CAGI	Compressed Air & Gas Institute
CAM	contract agreement manager
CEC	California Energy Commission
CEO	chief executive officer
CFD	computational fluid dynamics
CHNS	the elemental analysis of carbon, hydrogen, nitrogen, and sulfur concentrations in a given sample
dB	decibel
dBA	decibels A
F	Fahrenheit
FD2	Carnot Compression's prototype compressor model, the predecessor of the FD3
FD3	Carnot Compression's latest prototype compressor model, examined in this project
g	grams
g/s	grams per second
GTI	Gas Technology Institute, the project awardee
HP	horsepower
HVAC	heating, ventilation, and air conditioning
ISO	Independent System Operator
J	joule
K	kelvin

Term	Definition
kW	kilowatt
L	liter
lb_m	pounds mass, unit of mass equal to about 0.4536 kilograms
lb_m/s	pounds mass per second
LFE	laminar flow element
m	meter
M	mean
mg/L	milligrams per liter
mL	milliliter
mol	mole
NGV	The NGV World Podcast
NIOSH	National Institute of Occupational Safety and Health
NSF SBIR	National Science Foundation Small Business Innovation Research
OD	outside diameter
pH	potential hydrogen, the expression of the acidity or alkalinity of a solution on a logarithmic scale
PLC	programmable logic controller
psia	pounds per square inch, atmospheric
psig	pounds per square inch, gauge
RH	relative humidity
RERT	recirculation and energy recovery turbine
RTD	resistive temperature device
RPM	revolutions per minute
R^2	R squared
scfm	standard cubic feet per minute
SD	standard deviation
SU	standard unit
SVR	static vane return
umho/cm	micromhos per centimeter, a unit of electrical conductivity
W	watt
µg/L	micrograms per liter

References

Compressed Air & Gas Institute. (2021, January 12). Working with Compressed Air: Benefits: Costs. Retrieved from Compressed Air & Gas Institute: https://www.cagi.org/working-with-compressed-air/benefits/cost.aspx#!prettyPhoto

U.S. Department of Energy. (2022, April 6). 85 FR 1504 - Final Ruling. Energy Conservation Program: Energy Conservation Standards for Air Compressors. Retrieved April 6, 2022, from https://www.federalregister.gov/documents/2020/01/10/2019-26355/energy-conservation-program-energy-conservation-standards-for-air-compressors

Waide, P., and Brunner, C. (2011). Energy-Efficiency Policy Opportunities for Electric Motor-Driven Systems. IEA Energy Papers, No. 2011/07.